

## Non-Resonant Raman Optical Activity As Explored Via Phase-Space Electronic Structure Theory

Zhen Tao,<sup>1, a)</sup> Mansi Bhati,<sup>2</sup> and Joseph E. Subotnik<sup>2, b)</sup>

<sup>1)</sup>*Department of Chemistry, University of Rhode Island, Kingston, Rhode Island, 02881, USA*

<sup>2)</sup>*Department of Chemistry, Princeton University, Princeton, New Jersey 08544, USA*

In order to model experimental non-resonant Raman optical activity, chemists must compute a host of second-order response tensors, (e.g. the electric-dipole magnetic-dipole polarizability) and their nuclear derivatives. While these response functions are almost always computed along vibrational modes within a Born-Oppenheimer (BO) framework, here we provide a natural interpretation of the electric-dipole magnetic-dipole polarizability within phase space electronic structure theory, a beyond-BO model whereby the electronic structure depends on nuclear momentum ( $\mathbf{P}$ ) in addition to nuclear position ( $\mathbf{R}$ ). By coupling to nuclear momentum, phase space electronic structure theory is able to capture the asymmetric response of the electronic properties to an external field, insofar as *for a vibrating (non-stationary) molecule*,  $\frac{\partial \boldsymbol{\mu}}{\partial \mathbf{B}} \neq \frac{\partial \mathbf{m}}{\partial \mathbf{F}}$  where  $\boldsymbol{\mu}$  and  $\mathbf{m}$  are the electrical linear and magnetic dipoles, and  $\mathbf{F}$  and  $\mathbf{B}$  are electric and magnetic fields. As an example, for a prototypical methyloxirane molecule, we show that phase space electronic structure theory is able to deliver a reasonably good match with experimental results for a reasonable choice of gauge origin.

---

<sup>a)</sup>Electronic mail: zhen.tao@uri.edu

<sup>b)</sup>Electronic mail: js8441@princeton.edu

## I. INTRODUCTION

Chirality has important consequences with regards to biological protein recognition, and the capacity to influence the chirality forms the basis of major fields of research, including asymmetric catalysis for enantioselective synthesis,<sup>1–3</sup> chiral optoelectronics,<sup>4,5</sup> and biosensing for drug-target interactions.<sup>6,7</sup> Chirality has been more recently discovered to couple with electronic spins,<sup>8,9</sup> termed chiral-induced spin selectivity (CISS), which has important implications in spintronics,<sup>10</sup> electrocatalysis,<sup>11,12</sup> and possibly the origin of homochirality in life.<sup>13,14</sup>

At the most basic experimental level, chiral isomers can be distinguished by their difference in optical responses, so-called chiroptical spectroscopies. Circular dichroism (CD) is arguably the most common chiroptical technique, whereby one measures the difference in absorption of left-circularly polarized (LCP) light and right-circular polarized (RCP) light, and CD is usually studied in two distinct forms: electronic CD (ECD) which uses ultraviolet (UV) light to probe the electronic transitions and vibrational CD (VCD) which uses infrared (IR) light to probe the vibrational transitions. Apart from CD, Raman optical activity (ROA) is another means to measure chirality, whereby one measures the difference in Raman-scattered intensity of LCP and RCP light. Unlike VCD, ROA is particularly effective for samples in aqueous solutions because water has weak Raman signals, making ROA a powerful technique to study biomolecules such as proteins, carbohydrates, and nuclei acids in their natural aqueous solutions.<sup>15</sup> In practice, because Raman signals are weak, experimentalists often boost ROA signals by selectively coupling the electronic transition to vibrations and surface-enhanced Raman scattering.<sup>16–18</sup>

In this letter, our focus will be on ROA (as opposed to VCD). That being said, as will be made clear below, the motivation for the present article is to transfer advanced techniques from the theory of VCD over to the realm of ROA (see below). In that regard, a few preliminary words about VCD are especially pertinent at this juncture. (Interestingly, because the VCD and ROA signals are so weak, the theory behind both of these chiroptical spectroscopies were developed at roughly the same time as the experimental apparatuses themselves in the 1970s.<sup>19–21</sup>)

As a brief reminder, within VCD, when averaged over all incoming directions for the light, the rotational strength is  $\mathcal{R} = \hat{\boldsymbol{\mu}}_{i \rightarrow f}^{tot} \cdot \hat{\boldsymbol{m}}_{i \rightarrow f}^{tot}$ ,<sup>22,23</sup>. Here,  $\hat{\boldsymbol{\mu}}_{i \rightarrow f}^{tot}$  is the total, linear transition dipole moments (include both electronic and nuclear contributions);  $\hat{\boldsymbol{m}}_{i \rightarrow f}^{tot}$  is the total magnetic transition dipole moments (include both electronic and nuclear contributions). Note that, within standard quantum chemistry dogma, all vibrational spectroscopy (including VCD) is described in terms of

matrix elements between vibrationally excited states on a given Born-Oppenheimer (BO) electronic surface. Within such a BO approximation, all dynamic electron-nuclear correlation is ignored and the electronic component of the magnetic transition dipole vanishes,  $\hat{\mathbf{m}}_{i \rightarrow f}^e = 0$ . As a result, the computed VCD signals is proportional to the the magnetic moment from bare nuclear charges vibrating – which is completely wrong. In other words, a reasonable model of VCD spectroscopy mandates that one account dynamics on more than one BO surface. For going on three decades, the common solution to this is known as magnetic field perturbation theory,<sup>24–26</sup> which computes the necessary electronic atomic axial tensor (AAT) through a Berry curvature expression (see Eq. 38 below).<sup>27–29</sup> Here, the Berry curvature accounts for the additional electronic screening to the nuclear transition magnetic dipole moment and can be computed using several different BO calculations as input.

Now, in a recent paper,<sup>30</sup> our research group has demonstrated an alternative approach to VCD spectroscopy, whereby one can account for non-BO effects without computing the Berry curvature. Our approach was to completely avoid the BO framework and instead diagonalize an electronic phase space (PS) Hamiltonian<sup>31</sup> that captures the local dynamic electron–nuclear coupling via  $\mathbf{P} \cdot \hat{\mathbf{\Gamma}}$  term; here,  $\mathbf{P}$  is the nuclear momentum and  $\hat{\mathbf{\Gamma}}$  is an electronic operator that captures the local electronic momentum. For the form of the proposed  $\hat{\mathbf{\Gamma}}$  operator, see below (Eqs. 99 - 101); for a meaningful operator,  $\hat{\mathbf{\Gamma}}$  must satisfy the same four symmetry constraints as does the exact electron-nuclear derivative coupling operator.<sup>32</sup> See Eqs. 59-62 and Eqs. 65-68 below for these constraints. In practice, we have made progress by building a  $\hat{\mathbf{\Gamma}}$  operator that partitions space and lets electrons couple to nearby nuclear motion. As shown in Ref. 31, by working with a phase space Hamiltonian – that is parametrized by both  $\mathbf{R}$  and  $\mathbf{P}$  – we can naturally recover the non-zero electronic momentum dragged by nuclear motion. We can also recover reasonable electronic momentum and VCD signals.<sup>30,33</sup> Lastly, all of the theory above can be and has been extended to systems in the presence of an external magnetic field,<sup>34,35</sup> which introduces new physics as well.

At this point, let us return to ROA. According to standard time-dependent perturbation theory, the three key optical activity tensors that dictate ROA signals are the electric-dipole electric-dipole polarizability  $\alpha$ , the electric-dipole magnetic-dipole polarizability  $\mathbf{G}'$ , and the electric-dipole electric quadrupole polarizability  $\mathbf{A}$ . For practical computations of nonresonant ROA, the theory of ROA has historically made several approximations:

1. The molecular response to the electromagnetic fields is assumed to be linear, and one can calculate the relevant response function with BO theory through nuclear derivatives of the

Berry curvature.<sup>36</sup>

2. Nuclear vibrations are assumed to be harmonic.
3. In the static limit, the ROA tensors are assumed to be independent of the frequency of the incident light.
4. The ROA tensors are expanded to the first order in displacement with respect to the normal modes coordinates within the Placzek approximation<sup>37</sup>.
5. Many-body BO states are simplified to single-particle states.

One can go beyond these assumptions, including anharmonicity,<sup>38–40</sup> many-body effects through the more accurate treatment of electron-electron correlation,<sup>41,42</sup> and solvent effects,<sup>43,44</sup> but it must be noted that the theory of ROA is already quite difficult to implement and expensive to calculate (even more expensive than for VCD).<sup>45,46</sup>

With this background in mind, the motivation of the present article is clear. Our aim is to apply the phase space methods used in Ref. 30 for VCD theory to the realm of ROA spectroscopy. In particular, we will show that the electric-dipole magnetic-dipole polarizability  $\mathbf{G}'$  tensor can be expressed naturally within a phase space perspective, a notion that was hinted at previously by Escribano, Freedman, and Nafie<sup>47</sup>. Here we limit our discussion in the vibrational non-resonant ROA and we show direct determination of  $\mathbf{G}'$  through nuclear momentum dependence. An outline of this article is as follows: In Sec. II, we review the traditional way of computing the ROA tensor  $\mathbf{G}'$ . Thereafter, in Sec. III, we derive the PS framework to evaluate the ROA tensor  $\mathbf{G}'$ . In the results section, we show the ROA results obtained by the PS approach for a prototypical molecule, methyloxirane, and compare them to experiments and the traditional perturbation theory based on the BO states.

## II. STANDARD BERRY CURVATURE THEORY BASED ON BO THEORY

### A. Raman Optical Activity Tensors

Let us begin by briefly reviewing the conventional approach to evaluate the ROA tensors in the static limit. Ignoring all nuclear motion, the Hamiltonian describing the interaction of an

uncharged system in a time-dependent electric field  $\mathbf{F}$  can be written as

$$\hat{H} = \hat{H}_0 - \hat{\boldsymbol{\mu}} \cdot \mathbf{F} - \frac{1}{3} \sum_{\alpha\beta} \hat{\boldsymbol{\theta}}_{\alpha\beta} \nabla_{\beta} F_{\alpha} - \hat{\mathbf{m}} \cdot \mathbf{B} - \dots \quad (1)$$

Here  $\hat{H}_0$  is the electronic Hamiltonian in the absence of the external field.  $\mathbf{B}$  is the magnetic field associated with the external electric field. The responses for a quantum state  $\Psi_I$  (i.e. the electric dipole  $\boldsymbol{\mu}$ , the electric magnetic dipole  $\mathbf{m}$ , and the electric quadrupole  $\boldsymbol{\theta}$  as induced by the external fields) can be evaluated by time-dependent perturbation theory

$$\boldsymbol{\mu}_{\alpha}^{ind} = \sum_{\beta} \alpha_{\alpha\beta} F_{\beta} + \sum_{\beta} G_{\alpha\beta} B_{\beta} + \frac{1}{3} A_{\alpha,\beta\gamma} \nabla_{\beta} F_{\gamma} + \dots \quad (2)$$

$$\mathbf{m}_{\alpha}^{ind} = \sum_{\beta} \chi_{\alpha\beta} B_{\beta} + \sum_{\beta} G_{\beta\alpha}^* F_{\beta} + \dots \quad (3)$$

$$\boldsymbol{\theta}_{\alpha\beta}^{ind} = \sum_{\gamma} A_{\gamma,\alpha\beta} F_{\gamma} + \dots \quad (4)$$

Eqs. 2-4 introduce three key tensors that are necessary to calculate an ROA signal: the electric-dipole electric-dipole polarizability  $\boldsymbol{\alpha}$ , the electric-dipole magnetic-dipole polarizability  $\mathbf{G}$ , and the electric-dipole electric quadrupole polarizability  $\mathbf{A}$ . The corresponding sum-over-states expressions from the time-dependent perturbation theory are:

$$\alpha_{\alpha\beta} = \frac{2}{\hbar} \sum_{J \neq I} \frac{\omega_{JI}}{\omega_{JI}^2 - \omega^2} \text{Re} \left[ \langle \Psi_I | \hat{\mu}_{\alpha} | \Psi_J \rangle \langle \Psi_J | \hat{\mu}_{\beta} | \Psi_I \rangle \right] \quad (5)$$

$$G'_{\alpha\beta} = -\frac{2}{\hbar} \sum_{J \neq I} \frac{\omega}{\omega_{JI}^2 - \omega^2} \text{Im} \left[ \langle \Psi_I | \hat{\mu}_{\alpha} | \Psi_J \rangle \langle \Psi_J | \hat{m}_{\beta} | \Psi_I \rangle \right] \quad (6)$$

$$A_{\alpha\beta\gamma} = \frac{2}{\hbar} \sum_{J \neq I} \frac{\omega_{JI}}{\omega_{JI}^2 - \omega^2} \text{Re} \left[ \langle \Psi_I | \hat{\mu}_{\alpha} | \Psi_J \rangle \langle \Psi_J | \hat{\theta}_{\beta\gamma} | \Psi_I \rangle \right] \quad (7)$$

Here  $\hat{\mu}_{\alpha} = -e\hat{r}_{\alpha}$ ,  $\hat{m}_{\alpha} = -\frac{e}{2m_e}\hat{l}_{\alpha}$ , and  $\hat{\theta}_{\beta\gamma} = -e\left(\frac{3}{2}\hat{r}_{\beta}\hat{r}_{\gamma} - \frac{1}{2}\hat{r}^2\delta_{\beta\gamma}\right)$  are the electric dipole operator, the electric magnetic dipole operator, and the electric quadrupole operator, respectively.  $\omega$  is the frequency of the incoming light and  $\omega_{IJ}$  is the transition frequency between electronic states  $\Psi_I$  and  $\Psi_J$ .  $G'$  is the imaginary component of the electric-dipole magnetic-dipole polarizability  $\mathbf{G}$ . Note that the imaginary components of  $\boldsymbol{\alpha}$  and  $\mathbf{A}$  and the real component of  $\mathbf{G}$  are not included in the ROA tensors because the eigenstates of  $\hat{H}_0$  can be chosen to be real within the time-reversal symmetry.

In the static limit ( $\omega \rightarrow 0$ ), the electric-dipole electric-dipole polarizability  $\boldsymbol{\alpha}$  in Eq. 5, and

electric-dipole electric quadrupole polarizability  $\mathbf{A}$  in Eq. 7 become

$$\alpha_{\alpha\beta} = \frac{\partial \langle \Phi_I | \hat{\mu}_\beta | \Phi_I \rangle}{\partial F_\alpha} \quad (8)$$

$$A_{\alpha\beta\gamma} = \frac{\partial \langle \Phi_I | \hat{\theta}_{\beta\gamma} | \Phi_I \rangle}{\partial F_\alpha} \quad (9)$$

where  $\Phi_I$  is the perturbed wavefunction in an external electric field and magnetic field,

$$|\Phi_I\rangle = |\Psi_I\rangle - \sum_{J \neq I} \frac{\langle \Psi_J | \hat{\mu} \cdot \mathbf{F} | \Psi_I \rangle}{E_I - E_J} |\Psi_J\rangle - \sum_{J \neq I} \frac{\langle \Psi_J | \hat{m} \cdot \mathbf{B} | \Psi_I \rangle}{E_I - E_J} |\Psi_J\rangle \quad (10)$$

Eq. 10 follows for any hermitian operator from basic perturbation theory, so that  $\frac{\partial \langle \Phi_I | \hat{\theta} | \Phi_I \rangle}{\partial F_\alpha}$  has a natural sum-over-states form:

$$\frac{\partial \langle \Phi_I | \hat{\theta} | \Phi_I \rangle}{\partial F_\alpha} = - \sum_{J \neq I} \frac{\langle \Psi_I | \hat{\mu}_\alpha | \Psi_J \rangle}{E_I - E_J} \langle \Psi_J | \hat{\theta} | \Psi_I \rangle - \sum_{J \neq I} \langle \Psi_I | \hat{\theta} | \Psi_J \rangle \frac{\langle \Psi_J | \hat{\mu}_\alpha | \Psi_I \rangle}{E_I - E_J} \quad (11)$$

$$= \frac{2}{\hbar} \sum_{J \neq I} \frac{1}{\omega_{JI}} \text{Re} \left[ \langle \Psi_I | \hat{\mu}_\alpha | \Psi_J \rangle \langle \Psi_J | \hat{\theta}_\beta | \Psi_I \rangle \right] \quad (12)$$

For the electric-dipole magnetic-dipole polarizability  $\mathbf{G}'$ , one can find an expression without summing over states as follows. As suggested by Amos,<sup>36</sup> one can divide both sides of Eq. 6 by  $\omega$  and then take the static limit. In so doing, one arrives at the Berry-curvature-like expression

$$\omega^{-1} G'_{\alpha\beta} = -\frac{2}{\hbar} \sum_{J \neq I} \frac{1}{\omega_{JI}^2} \text{Im} \left[ \langle \Psi_I | \hat{\mu}_\alpha | \Psi_J \rangle \langle \Psi_J | \hat{m}_\beta | \Psi_I \rangle \right] \quad (13)$$

$$= -2\hbar \text{Im} \left\langle \frac{\partial \Phi_I}{\partial F_\alpha} \middle| \frac{\partial \Phi_I}{\partial B_\beta} \right\rangle \quad (14)$$

To obtain Eq.14 from Eq.13, one can write out the derivatives of the perturbed wavefunction in Eq. 10 with respect to the external magnetic and electric field,

$$\left| \frac{\partial \Phi_I}{\partial B_\alpha} \right\rangle = - \sum_{J \neq I} \frac{\hat{m}_{JI}^\alpha}{E_I - E_J} |\Psi_J\rangle \quad (15)$$

$$\left\langle \frac{\partial \Phi_I}{\partial F_\alpha} \right| = - \sum_{J \neq I} \frac{\hat{\mu}_{IJ}^\alpha}{E_I - E_J} \langle \Psi_J | \quad (16)$$

As mentioned above, in order to calculate non-resonant vibrational Raman optical activity, one must evaluate all three response tensors above when sandwiched between the ground vibrational state and an excited vibrational state. To that end, it is standard today to invoke the BO approximation, where the total molecular wavefunction is written as a product of nuclear vibrational state and electronic state  $\Psi_I(\mathbf{R}, \mathbf{r}) = \psi_I(\mathbf{r}; \mathbf{R})\chi(\mathbf{R})$ . Thereafter, for a given vibrational mode  $k$ , the

polarizability tensors can be expanded in the molecular normal mode coordinates  $\mathbf{Q}$  based on the Placzek's approximation. For example, the the electric-dipole magnetic-dipole polarizability  $\mathbf{G}'$  becomes

$$\omega^{-1} G_{\alpha\beta}^{\prime k} = \omega^{-1} \frac{\partial G_{\alpha\beta}}{\partial Q_k} \langle \chi_0^{(k)} | \mathbf{Q}_k | \chi_1^{(k)} \rangle \quad (17)$$

$$= \omega^{-1} \frac{\partial G_{\alpha\beta}}{\partial \mathbf{R}} \Big|_{\mathbf{Q}=0} \cdot \mathbf{S}_k \langle \chi_0^{(k)} | \mathbf{Q}_k | \chi_1^{(k)} \rangle \quad (18)$$

$$= -2\hbar \left( \frac{\hbar}{2\omega_k} \right)^{\frac{1}{2}} \frac{\partial}{\partial \mathbf{R}} \text{Im} \left\langle \frac{\partial \psi_I}{\partial F_\alpha} \Big| \frac{\partial \psi_I}{\partial B_\beta} \right\rangle \Big|_{\mathbf{Q}=0} \cdot \mathbf{S}_k \quad (19)$$

Here  $\mathbf{S}_k = \frac{\partial \mathbf{R}}{\partial Q_k} \Big|_{\mathbf{Q}=0}$  describes the Cartesian nuclear displacements in normal mode  $k$  and

$$\langle \chi_0^{(k)} | \mathbf{Q}_k | \chi_1^{(k)} \rangle = \langle \chi_1^{(k)} | \mathbf{Q}_k | \chi_0^{(k)} \rangle = \left( \frac{\hbar}{2\omega_k} \right)^{\frac{1}{2}} \quad (20)$$

are the standard position operator matrix elements for a harmonic oscillator.

## B. Circular Intensity Difference

Experimental ROA intensities routinely measure the dimensionless circular intensity difference (CID)

$$\Delta_\alpha = \frac{I_\alpha^R - I_\alpha^L}{I_\alpha^R + I_\alpha^L}, \quad (21)$$

where  $I_\alpha^R$  and  $I_\alpha^L$  are the scattered Raman intensities for a molecule subjected to right- and left-circularly polarized excitation, respectively, and the scattered light is analyzed in a linear polarization defined by the analyzer angle  $\alpha$  with respect to the chosen reference.<sup>48</sup> The CID expressions for different experimental setups with incident light of wavelength  $\lambda$  have been listed in terms of ROA invariants in Ref. 49 and are also listed in Table I here.

In Table I above, several ROA invariants have been calculated from the polarizabilities in Eqs.

TABLE I. Relevant expressions for circular intensity difference under different measurement types.

Measurement type	$\Delta = \frac{I^R - I^L}{I^R + I^L}$
Depolarized	$\frac{4\pi}{\lambda} \left[ \frac{\gamma^2}{\omega} - \frac{1}{3} \frac{\delta^2}{\omega} \right] / \beta^2$
Polarized	$\frac{4\pi}{\lambda} \left[ \frac{45}{\omega} \alpha G' + \frac{7}{\omega} \gamma^2 + \frac{1}{\omega} \delta^2 \right] / [45\alpha^2 + 7\beta^2]$
Magic angle	$\frac{4\pi}{\lambda} \left[ \frac{9}{\omega} \alpha G' + \frac{2}{\omega} \gamma^2 \right] / [9\alpha^2 + 2\beta^2]$
Backward	$\frac{48\pi}{\lambda} \left[ \frac{1}{\omega} \gamma_j^2 + \frac{1}{3\omega} \delta^2 \right] / [45\alpha^2 + 7\beta^2]$
Forward	$\frac{48\pi}{\lambda} \left[ \frac{45}{\omega} \alpha G' + \frac{1}{\omega} \gamma^2 - \frac{1}{\omega} \delta^2 \right] / [45\alpha^2 + 7\beta^2]$

8, 9, and 14.

$$\alpha^2 = \frac{1}{9} \sum_{\alpha\beta} \alpha_{\alpha\alpha} \alpha_{\beta\beta} \quad (22)$$

$$\beta^2 = \frac{1}{2} \sum_{\alpha\beta} (3\alpha_{\alpha\beta} \alpha_{\alpha\beta} - \alpha_{\alpha\beta} \alpha_{\beta\beta}) \quad (23)$$

$$\alpha G' = \frac{1}{9} \sum_{\alpha\alpha} \alpha_{\alpha\alpha} G'_{\beta\beta} \quad (24)$$

$$\gamma^2 = \frac{1}{2} \sum_{\alpha\alpha} (3\alpha_{\alpha\beta} G'_{\alpha\beta} - \alpha_{\alpha\alpha} G'_{\beta\beta}) \quad (25)$$

$$\delta^2 = \frac{1}{2} \omega \sum_{\alpha\beta} \alpha_{\alpha\beta} \sum_{\gamma\delta} \varepsilon_{\alpha\gamma\delta} A_{\gamma\delta\beta} \quad (26)$$

For magic-angle measurements, the predicted ROA CID Table I and the final result is:

$$\Delta_{BO}^k(*) = \frac{4\pi}{\lambda} \left[ \sum_{\alpha\beta} \frac{\partial \alpha_{\alpha\beta}}{\partial Q_k} \frac{\omega_k^{-1} \partial G'_{\alpha\beta}}{\partial Q_k} \right] / \left[ \sum_{\alpha\beta} \frac{\partial \alpha_{\alpha\beta}}{\partial Q_k} \frac{\partial \alpha_{\alpha\beta}}{\partial Q_k} \right] \quad (27)$$

Similar formulas can be found for the other CID expressions. Henceforward, given that Table I involves  $\omega^{-1} G'$ , for which there is a the Berry curvature expression (Eq. 14), we will refer to Table I above as either BO or Berry curvature ROA expressions.

### III. PHASE SPACE THEORY OF ROA

As far as predicting ROA signals, the key element above is the  $\omega^{-1} \frac{\partial G'_{\gamma\alpha}}{\partial \mathbf{R}}$  term in Eq. 27. Interestingly, the matrix element  $\omega^{-1} \frac{\partial G'_{\gamma\alpha}}{\partial \mathbf{R}}$  can be reintrepreted through phase space theory, which

we will now discuss.

### A. Brief Review of Shenvi’s Phase Space Electronic Structure Theory

As was established long ago by many chemists (including Nafie<sup>50</sup>, Stephens<sup>24</sup>, and Patchkovski<sup>51</sup>), in the context of chiroptical spectroscopy, the main failure of BO theory is the lack of any dependence of the nuclear momentum for the electronic wave function. After all, within the BO approximation, one discards the term

$$\hat{H}' = -i\hbar \sum_{IJ} \frac{\mathbf{P} \cdot \mathbf{d}_{IJ}}{M} |\psi_I\rangle \langle \psi_J| \quad (28)$$

Here  $\mathbf{d}_{IJ} = \langle \psi_I | \frac{\partial}{\partial \mathbf{R}} | \psi_J \rangle$  is the derivative coupling vector and  $\hat{H}'$  can be considered the first-order correction to BO theory. As a result of ignoring the coupling in Eq. 28 above BO lacks electronic momentum<sup>52–54</sup> and cannot predict VCD theory directly (among other ailments).<sup>30,50,51,55</sup>

Now, in 2008, Shenvi tried to incorporate this nuclear momentum dependence back to electronic states by diagonalizing the molecular Hamiltonian in the adiabatic basis to obtain superadiabatic states.<sup>56</sup>

$$\hat{H}_{\text{Shenvi}}(\mathbf{R}, \mathbf{P}) = \sum_{IJK,A} \frac{1}{2M_A} \left( P_A \delta_{IJ} - i\hbar \mathbf{d}_{IJ}^A \right) \cdot \left( P_A \delta_{JK} - i\hbar \mathbf{d}_{JK}^A \right) |\psi_I\rangle \langle \psi_K| + \sum_K E_K(\mathbf{R}) |\psi_K\rangle \langle \psi_K|, \quad (29)$$

This formalism, however, is not practically stable due to the well-known diverging character of derivative coupling vectors near avoided crossings and high computational expense of computing derivative couplings in the select subspace of adiabatic states. Furthermore, derivative couplings are known to be gauge dependent, which are not well defined in the presence of degenerate states. Despite these failures, however, it is worth noting that Shenvi’s approach does provide an interpretation of Eq. 14 above, which we now discuss.

### B. Interpretation of $G'$ tensor in terms of Nuclear Momentum Dependence

Let us begin by recapitulating<sup>30,50</sup> how and why an electronic wavefunction depends on nuclear momentum, and how such dependence allows us to calculate the AAT (Eq. 38) for VCD calculations; thereafter, we will show how one can similarly express  $\omega^{-1} \frac{\partial G'_{\gamma\alpha}}{\partial \mathbf{R}}$  in terms of derivatives with respect to nuclear momentum within phase space theory. If one considers the term

$-i\hbar \sum_{IJ} \frac{\mathbf{P} \cdot \mathbf{d}_{IJ}}{M} |\psi_I\rangle \langle \psi_J|$  as a perturbation on top of BO theory, then within phase space electronic structure theory, the nuclear momentum dependence of the electronic wavefunction can also be written in a perturbative way:

$$|\Phi_I^P\rangle = |\psi_I\rangle - i\hbar \sum_{J \neq I} \frac{\sum_A \frac{\mathbf{P}^A}{M_A} \cdot \mathbf{d}_{JI}^A}{E_I - E_J} |\psi_J\rangle \quad (30)$$

$$= |\psi_I\rangle - i\hbar \sum_{J \neq I} \frac{\sum_A \frac{\mathbf{P}^A}{M_A} \cdot \langle \psi_J | \frac{\partial \hat{H}}{\partial \mathbf{R}_A} | \psi_I \rangle}{(E_I - E_J)^2} |\psi_J\rangle \quad (31)$$

Thus, if we differentiate an electronic wavefunction derivative with respect to the nuclear momentum, we find:

$$\left| \frac{\partial \Phi_I^P}{\partial \mathbf{P}_A} \right\rangle = -i\hbar \sum_{J \neq I} \frac{1}{M_A} \frac{d_{JI}^A}{E_I - E_J} |\psi_J\rangle = -i\hbar \sum_{J \neq I} \frac{1}{M_A} \frac{\langle \psi_J | \frac{\partial \hat{H}}{\partial \mathbf{R}_A} | \psi_I \rangle}{(E_I - E_J)^2} |\psi_J\rangle \quad (32)$$

Similarly, we can write down the dependence of the electronic wavefunction on the nuclear displacement

$$|\Phi_I^R\rangle = |\psi_I\rangle + \sum_{J \neq I} \frac{\sum_{A\alpha} \langle \psi_J | \frac{\partial \hat{H}}{\partial R_{A\alpha}} | \psi_I \rangle \delta R_{A\alpha}}{E_I - E_J} |\psi_J\rangle \quad (33)$$

and the wavefunction derivative with respect to the nuclear displacement

$$\left| \frac{\partial \Phi_I^R}{\partial R_{A\alpha}} \right\rangle = \sum_{J \neq I} \frac{\langle \psi_J | \frac{\partial \hat{H}}{\partial R_{A\alpha}} | \psi_I \rangle}{E_I - E_J} |\psi_J\rangle \quad (34)$$

Combining Eq.15, Eq. 32, and Eq.34, we can derive the AAT expression based on the magnetic field perturbation theory<sup>24</sup>

$$\frac{\partial \langle \Phi_I^P | \hat{m}_\alpha | \Phi_I^P \rangle}{\partial P_{A\beta}} = \left\langle \frac{\partial \Phi_I^P}{\partial P_{A\beta}} \left| \hat{m}_\alpha \right| \Phi_I^P \right\rangle + \left\langle \Phi_I^P \left| \hat{m}_\alpha \right| \frac{\partial \Phi_I^P}{\partial P_{A\beta}} \right\rangle \quad (35)$$

$$= -i\hbar \sum_{J \neq I} \frac{1}{M_A} \frac{\langle \psi_I | \frac{\partial \hat{H}}{\partial R_{A\beta}} | \psi_J \rangle}{(E_I - E_J)^2} \langle \psi_J | \hat{m}_\alpha | \psi_I \rangle - i\hbar \sum_{J \neq I} \frac{1}{M_A} \frac{\langle \psi_J | \frac{\partial \hat{H}}{\partial R_{A\beta}} | \psi_I \rangle}{(E_I - E_J)^2} \langle \psi_I | \hat{m}_\alpha | \psi_J \rangle \quad (36)$$

$$= \frac{2\hbar}{M_A} \text{Im} \left[ \sum_{J \neq I} \frac{\langle \psi_J | \frac{\partial \hat{H}}{\partial R_{A\beta}} | \psi_I \rangle}{(E_I - E_J)^2} \langle \psi_I | \hat{m}_\alpha | \psi_J \rangle \right] \quad (37)$$

$$= -\frac{2\hbar}{M_A} \text{Im} \left\langle \frac{\partial \Phi_I}{\partial B_\alpha} \left| \frac{\partial \Phi_I}{\partial R_\beta} \right\rangle \quad (38)$$

Differentiating the AAT with respect to the external electric field yields

$$\frac{\partial^2 \langle \Phi_I^P | \hat{m}_\alpha | \Phi_I^P \rangle}{\partial F_\gamma \partial P_\beta} = -\frac{2\hbar}{M} \frac{\partial}{\partial F_\gamma} \text{Im} \left\langle \frac{\partial \Phi_I}{\partial B_\alpha} \middle| \frac{\partial \Phi_I}{\partial R_\beta} \right\rangle \quad (39)$$

Note that one must go beyond the BO approximation to include electron–nuclear momentum coupling in Eq.31 to find a non-zero AAT.<sup>30,50</sup>

Similarly, from the same wavefunction perturbations in Eq.16, Eq. 32, and Eq.34, one can write down

$$\frac{\partial^2 \langle \Phi_I^P | \hat{\mu}_\gamma | \Phi_I^P \rangle}{\partial B_\alpha \partial P_\beta} = -\frac{2\hbar}{M} \frac{\partial}{\partial B_\alpha} \text{Im} \left\langle \frac{\partial \Phi_I}{\partial F_\gamma} \middle| \frac{\partial \Phi_I}{\partial R_\beta} \right\rangle \quad (40)$$

As above, this term will be zero within the BO approximation as there is no nuclear momentum dependence of the electronic wavefunction even in the presence of an external magnetic field.

Now we introduce a new definition.

$$W_{\gamma\alpha}(\mathbf{R}, \mathbf{P}) = \frac{\partial \langle \Phi_I^P | \hat{\mu}_\gamma | \Phi_I^P \rangle}{\partial B_\alpha} - \frac{\partial \langle \Phi_I^P | \hat{m}_\alpha | \Phi_I^P \rangle}{\partial F_\gamma} \quad (41)$$

Note that the wavefunction  $\Phi_I^P$  is the perturbed wavefunction arising from the perturbing nonadiabatic operator  $-i\hbar \frac{\mathbf{P}}{M} \cdot \hat{\mathbf{d}}$ , which reduces to BO wavefunction when  $\mathbf{P} = 0$ . The newly introduced tensor  $W_{\gamma\alpha}$  is only non-zero at  $\mathbf{P} \neq 0$  and represents the asymmetry of the second-order electronic responses when the nuclei are moving (so as to break time-reversal symmetry). In other words, within BO theory (which is nearly equivalent to phase space theory when  $\mathbf{P} = 0$  up to a second-order term in  $\mathbf{d}_{IJ}$ ), for arbitrary  $\mathbf{B}$  and  $\mathbf{F}$  fields and position  $\mathbf{R}$ ,

$$\langle \psi | \hat{m} | \psi \rangle = -\langle \psi | \frac{\partial \hat{H}}{\partial \mathbf{B}} | \psi \rangle = -\frac{\partial \langle \psi | \hat{H} | \psi \rangle}{\partial \mathbf{B}} \approx -\frac{\partial \langle H_{Shemvi} \rangle}{\partial \mathbf{B}} \Big|_{\mathbf{P}=0} \quad (42)$$

$$\langle \psi | \hat{\mu} | \psi \rangle = -\langle \psi | \frac{\partial \hat{H}}{\partial \mathbf{F}} | \psi \rangle = -\frac{\partial \langle \psi | \hat{H} | \psi \rangle}{\partial \mathbf{F}} \approx -\frac{\partial \langle H_{Shemvi} \rangle}{\partial \mathbf{F}} \Big|_{\mathbf{P}=0} \quad (43)$$

so that the  $\mathbf{W}$  tensor must be exactly zero:

$$\frac{\partial \langle \psi | \hat{\mu}_\gamma | \psi \rangle}{\partial B_\alpha} = -\frac{\partial^2 \langle \psi | \hat{H} | \psi \rangle}{\partial F_\gamma \partial B_\alpha} = \frac{\partial \langle \psi | \hat{m}_\alpha | \psi \rangle}{\partial F_\gamma} \quad (44)$$

However, while we are free to differentiate Eq. 44 with respect to nuclear positions  $\mathbf{R}$ , so that

$$\frac{\partial^2 \langle \psi | \hat{\mu}_\gamma | \psi \rangle}{\partial R_{A\beta} \partial B_\alpha} = \frac{\partial^2 \langle \psi | \hat{m}_\alpha | \psi \rangle}{\partial R_{A\beta} \partial F_\gamma} \quad (45)$$

we cannot take such derivatives with respect to nuclear momentum  $\mathbf{P}$  (where we necessarily must go beyond BO theory):

$$\frac{\partial^2 \langle \Phi^P | \hat{\mu}_\gamma | \Phi^P \rangle}{\partial P_{A\beta} \partial B_\alpha} \neq \frac{\partial^2 \langle \Phi^P | \hat{m}_\alpha | \Phi^P \rangle}{\partial P_{A\beta} \partial F_\gamma} \quad (46)$$

In other words, if  $\mathbf{P} \neq 0$ ,

$$\frac{\partial \langle \Phi^P | \hat{\mu}_\gamma | \Phi^P \rangle}{\partial B_\alpha} \neq \frac{\partial \langle \Phi^P | \hat{m}_\alpha | \Phi^P \rangle}{\partial F_\gamma} \quad (47)$$

These relationships break down because, by allowing electrons to move with nuclei, a nonzero electronic angular momentum ( $\mathbf{m}$ ) can arise both from internal nuclear motion  $\mathbf{P}$  and an external magnetic field  $\mathbf{B}$ , so that Eq. 44 holds only when  $\mathbf{P} = 0$ . See below, Sec. IIID, for a complete analysis of this term within phase space theory.

Taking the derivative of  $W_{\gamma\alpha}$  with respect to nuclear momentum, one arrives at the the ROA tensor  $\omega^{-1} \frac{\partial G'_{\gamma\alpha}}{\partial \mathbf{R}}$

$$\frac{\partial W_{\gamma\alpha}}{\partial \mathbf{P}_\beta} = \frac{\partial^2 \langle \Phi_I^P | \hat{\mu}_\gamma | \Phi_I^P \rangle}{\partial B_\alpha \partial \mathbf{P}_\beta} - \frac{\partial^2 \langle \Phi_I^P | \hat{m}_\alpha | \Phi_I^P \rangle}{\partial F_\gamma \partial \mathbf{P}_\beta} \quad (48)$$

$$= \frac{2\hbar}{M} \text{Im} \left[ \left\langle \frac{\partial \Psi_I}{\partial B_\alpha} \left| \frac{\partial^2 \Psi_I}{\partial F_\gamma \partial R_\beta} \right. \right\rangle - \left\langle \frac{\partial \Psi_I}{\partial F_\gamma} \left| \frac{\partial^2 \Psi_I}{\partial B_\alpha \partial R_\beta} \right. \right\rangle \right] \quad (49)$$

$$= \frac{2\hbar}{M} \text{Im} \left[ \left\langle \frac{\partial \Psi_I}{\partial B_\alpha} \left| \frac{\partial^2 \Psi_I}{\partial F_\gamma \partial R_\beta} \right. \right\rangle + \left\langle \frac{\partial^2 \Psi_I}{\partial B_\alpha \partial R_\beta} \left| \frac{\partial \Psi_I}{\partial F_\gamma} \right. \right\rangle \right] \quad (50)$$

$$= \frac{2\hbar}{M} \frac{\partial}{\partial \mathbf{R}} \text{Im} \left\langle \frac{\partial \Psi_I}{\partial B_\alpha} \left| \frac{\partial \Psi_I}{\partial F_\gamma} \right. \right\rangle \quad (51)$$

$$= \frac{1}{M} \omega^{-1} \frac{\partial G'_{\gamma\alpha}}{\partial \mathbf{R}} \quad (52)$$

Therefore the electric-dipole magnetic-dipole polarizability  $\mathbf{G}'$  in Eq.19 can be calculated alternatively by evaluating the changes with respect to conjugate momentum  $\Pi_k$  for a given normal mode  $k$ .

$$\omega^{-1} G'_{\alpha\beta} = \frac{\partial W_{\alpha\beta}}{\partial \Pi_k} \langle \chi_0^{(k)} | \Pi_k | \chi_1^{(k)} \rangle \quad (53)$$

$$= \frac{\partial W_{\alpha\beta}}{\partial \mathbf{P}} \Big|_{\Pi=0} \cdot \mathbf{S}_k \langle \chi_0^{(k)} | \Pi_k | \chi_1^{(k)} \rangle \quad (54)$$

$$= -i \left( \frac{\hbar \omega_k}{2} \right)^{\frac{1}{2}} M \frac{\partial W_{\alpha\beta}}{\partial \mathbf{P}} \Big|_{\Pi=0} \cdot \mathbf{S}_k \quad (55)$$

$$= \left( \frac{\hbar \omega_k}{2} \right)^{\frac{1}{2}} M \text{Im} \frac{\partial W_{\alpha\beta}}{\partial \mathbf{P}} \Big|_{\Pi=0} \cdot \mathbf{S}_k \quad (56)$$

To go from Eq. 54 to Eq. 56, we evaluate the matrix element for the harmonic oscillator momentum operator  $\langle \chi_0^{(k)} | \Pi_k | \chi_1^{(k)} \rangle = -\langle \chi_1^{(k)} | \Pi_k | \chi_0^{(k)} \rangle = -i \left( \frac{\hbar \omega_k}{2} \right)^{\frac{1}{2}} M$ .

The  $\mathbf{G}'$  tensor, and hence the CID signals can be calculated with both approaches (Eq. 19 and Eq. 56). As an example, for magic angle CID, for a given vibrational transition from ground to

kth vibrational state, the result is:

$$\Delta_{PS}^k(*) = -\frac{4i\pi}{\lambda\omega_k} \left[ \sum_{\alpha\beta} \frac{\partial\alpha_{\alpha\beta}}{\partial Q_k} \frac{\partial W_{\gamma\alpha}}{\partial \Pi_k} \right] / \left[ \sum_{\alpha\beta} \frac{\partial\alpha_{\alpha\beta}}{\partial Q_k} \frac{\partial\alpha_{\alpha\beta}}{\partial Q_k} \right] \quad (57)$$

### C. A More Practical Theory of Phase Space Electronic Structure Theory

The theory above makes clear that ROA can be explained naturally in the context of an electronic structure theory parameterized by both  $\mathbf{R}$  and  $\mathbf{P}$ . That being said, at the end of Sec. III A, we argued that the Shenvi approach in Eq. 29 was not optimal. Thus, to make further progress, one must be prepared to make approximations. To that end, over the last few years, our research groups have proposed an electronic phase-space Hamiltonian, where we approximate the non-diverging part of the derivative coupling with a one-electron  $\hat{\Gamma}$  operator.<sup>31</sup>

$$\hat{H}_{PS}(\mathbf{R}, \mathbf{P}) = \sum_A \frac{1}{2M_A} (\mathbf{P}_A - i\hbar\hat{\Gamma}_A(\mathbf{R})) \cdot (\mathbf{P}_A - i\hbar\hat{\Gamma}_A(\mathbf{R})) + \hat{H}_{el}(\mathbf{R}), \quad (58)$$

The nuclear-momentum coupling term  $-i\hbar\frac{\mathbf{P}}{M} \cdot \hat{\Gamma}$  can be viewed as the surrogate first-order correction<sup>57</sup> beyond the BO approximation, provided  $\hat{\Gamma}$  approximates the derivative coupling operator. The key question is then how to construct  $\hat{\Gamma}$  exactly.

#### 1. Field Free Phase Space Electronic Structure Theory

In the absence of a magnetic field, the derivative coupling operator  $d_{JK}^A$  satisfies (for  $J \neq K$ ) the symmetries listed below in Eqs. 59-62.<sup>32</sup>

$$-i\hbar \sum_A d_{JK}^A + \langle \psi_J | \hat{\mathbf{p}} | \psi_K \rangle = 0, \quad (59)$$

$$\sum_I \nabla_A d_{JK}^A = 0, \quad (60)$$

$$-i\hbar \sum_A \mathbf{R}_A \times d_{JK}^A + \langle \psi_J | \hat{\mathbf{l}} + \hat{\mathbf{s}} | \psi_K \rangle = 0, \quad (61)$$

$$-\sum_A \left( \mathbf{R}_A \times \nabla_A d_{JK}^{B\beta} \right)_\alpha = \sum_\gamma \varepsilon_{\alpha\beta\gamma} d_{JK}^{B\gamma}, \quad (62)$$

Because electrons move together with nuclear translation, summing over all the nuclear contribution to the derivative coupling vector between states  $J$  and  $K$  equals to the electronic linear momentum between those two states  $\mathbf{p}_{JK}$ , as shown in Eq. 59. Similar relation is presented in Eq.

61 for rigid rotation which equates the total nuclear angular momentum to the total electronic angular momentum operator  $\hat{\mathbf{l}} + \hat{\mathbf{s}}$ . Of course, the derivative coupling is not well-defined for  $J = K$  and really amounts to a choice of phase convention. As argued by Littlejohn *et al.*,<sup>58</sup> the most natural phase convention is to choose:

$$\left(\hat{\mathbf{P}}_N + \hat{\mathbf{p}}\right)\psi(\mathbf{r}, \mathbf{R}) = 0 \quad (63)$$

$$\left(\hat{\mathbf{J}}_N + \hat{\mathbf{j}}\right)\psi(\mathbf{r}, \mathbf{R}) = 0 \quad (64)$$

which are automatically consistent with Eqs. 59 and 61 for  $J \neq K$ . Here  $\hat{\mathbf{P}} = -i\hbar \sum_A \frac{\partial}{\partial \mathbf{R}_A}$ . Altogether, if we now extrapolate these symmetry relations for a one-electron operator  $\hat{\Gamma}$ , we postulate the resulting operator should satisfy the following corresponding symmetries:<sup>31</sup>

$$-i\hbar \sum_A \hat{\Gamma}_A + \hat{\mathbf{p}} = 0, \quad (65)$$

$$\left[-i\hbar \sum_B \frac{\partial}{\partial \mathbf{R}_B} + \hat{\mathbf{p}}, \hat{\Gamma}_A\right] = 0, \quad (66)$$

$$-i\hbar \sum_A \mathbf{R}_A \times \hat{\Gamma}_A + \hat{\mathbf{l}} + \hat{\mathbf{s}} = 0, \quad (67)$$

$$\left[-i\hbar \sum_B \left(\mathbf{R}_B \times \frac{\partial}{\partial \mathbf{R}_B}\right)_\gamma + \hat{l}_\gamma + \hat{s}_\gamma, \hat{\Gamma}_{A\delta}\right] = i\hbar \sum_\alpha \varepsilon_{\alpha\gamma\delta} \hat{\Gamma}_{A\alpha}, \quad (68)$$

The constraints in Eqs. 65 and 67 partition the electronic linear momentum and angular momentum to each moving nucleus to conserve total (nuclear+electronic) linear and angular momentum. In this paper, we focus on systems lacking net spin and therefore omit the spin operator  $\hat{\mathbf{s}}$  from the definition of  $\hat{\Gamma}$  henceforth. The constraints in Eqs. 66 and 68 ensure the phase space energy is invariant to molecular translation and rotation, respectively.<sup>31</sup>

Following these symmetry constraints, we have previously designed a one-electron  $\hat{\Gamma}$  operator<sup>31</sup> consisting of an electron translational factor (ETF)  $\hat{\Gamma}'$ <sup>59,60</sup> and an electron rotational factor (ERF)  $\hat{\Gamma}''$ .<sup>61,62</sup>

$$\hat{\Gamma}_A = \hat{\Gamma}'_A + \hat{\Gamma}''_A \quad (69)$$

$$\hat{\Gamma}'_A = \frac{1}{2i\hbar} (\hat{\Theta}_A(\hat{\mathbf{r}})\hat{\mathbf{p}}_A + \hat{\mathbf{p}}_A\hat{\Theta}_A(\hat{\mathbf{r}})) \quad (70)$$

$$\hat{\Gamma}''_A = \sum_B \zeta_{AB} (\mathbf{R}_A - \mathbf{R}_B^0) \times \left( \mathbf{K}_B^{-1} \frac{1}{2i\hbar} (\hat{\mathbf{r}} - \mathbf{R}_B) \times (\hat{\Theta}_B(\hat{\mathbf{r}})\hat{\mathbf{p}}_B + \hat{\mathbf{p}}_B\hat{\Theta}_B(\hat{\mathbf{r}})) \right) \quad (71)$$

The ETF term involves a partition-of-unity operator  $\hat{\Theta}$  in the real three-dimensional space to partition the electron-nuclear coupling regions under the translational-type of nuclear motion.

$$\Theta_A(\hat{\mathbf{r}}) = \frac{eQ_A e^{-|\hat{\mathbf{r}}-\mathbf{R}_A|^2/\sigma^2}}{\sum_B eQ_B e^{-|\hat{\mathbf{r}}-\mathbf{R}_B|^2/\sigma^2}}. \quad (72)$$

Here the prefactors  $Q_A$  are the bare nuclear charges of nuclei A and  $\sigma$  is a locality parameter that controls the width of the electronic-nuclear momentum couplings. The ERF term  $\hat{\Gamma}''$  includes another locality function  $\zeta$  that partition the regions of coupling for the rotational-type of motion with a locality parameter  $\beta$ .

$$\zeta_{AB} = M_A e^{-|\mathbf{R}_A-\mathbf{R}_B|^2/\beta^2} \quad (73)$$

Although the exact symmetry constraints above do not uniquely define the form of  $\hat{\Gamma}$ , we have demonstrated that the choice of  $\hat{\Gamma}$  in Eqs.69 -71 is reasonable by benchmarking several quantities, such as electronic momentum, electronic current densities, and vibrational circular dichroism.<sup>30,31,33</sup>

At this point, however, it is crucial to note that, for evaluating Eq.56 above, we must work *in the presence* of a magnetic field. To compute the ROA tensors in Eq. 57, we need to explicitly take into account the effects of an external magnetic field.

## 2. Phase Space Electronic Structure Theory in the Presence of External Magnetic Fields

Before we address the proper theory of phase space electronic structure in the presence of a uniform magnetic field, let us remind the reader extremely briefly about dynamics in the presence of a  $\mathbf{B}$  field. In the presence of a magnetic field, both the nuclei and electrons experience the magnetic field. Within the BO framework, the total Hamiltonian can be separated naturally as follows:

$$\hat{H}_{\text{BO}}^{\text{mag}}(\mathbf{R}, \mathbf{B}) = \sum_A \frac{\Pi_A^2(\mathbf{B})}{2M_A} + \hat{H}_{\text{el}}^{\text{mag}}(\mathbf{R}, \mathbf{B}), \quad (74)$$

$$\hat{H}_{\text{el}}^{\text{mag}}(\mathbf{R}, \mathbf{B}) = \sum_i \frac{\hat{\pi}_i^2}{2} + \hat{V}_{eN} + \hat{V}_{ee} + \hat{V}_{NN} \quad (75)$$

Here the nuclear and electronic kinetic (as opposed to canonical) momentum are

$$\Pi_A = \mathbf{P}_A - Q_A e \mathbf{A}(\mathbf{R}_A) \quad (76)$$

$$\boldsymbol{\pi}_i = \mathbf{p}_i + e \mathbf{A}(\mathbf{r}_i) \quad (77)$$

Above,  $\mathbf{A}(\mathbf{R}) = \frac{1}{2}\mathbf{B} \times (\mathbf{R} - \mathbf{G}_0)$  is the vector potential of the external magnetic field  $\mathbf{B}$  at position  $\mathbf{R}$  with a gauge origin at  $\mathbf{G}_0$ . Two points are worth noting at this juncture: (i) The magnetic field in the total Hamiltonian appears only in the kinetic momentum, which makes the entire theory gauge invariant (i.e., all dynamics will be invariant to the choice of  $\mathbf{G}$ ). (ii) As pointed out in Refs. 63–65, if one runs dynamics along an eigensurface of Eq. 75, unfortunately, the resulting description lacks electronic shielding; nuclei experience the external magnetic fields as bare nuclear charges (whereas in truth, nuclei always drag an electronic cloud). To capture the missing electronic shielding, it is well-understood that the Berry connection or the diagonal component of the derivative coupling vector has to be included.

$$\hat{H}_{\text{ad}}^{\text{mag}}(\mathbf{R}, \mathbf{B}) = \sum_A \frac{(\Pi_A(\mathbf{B}) - i\hbar \hat{d}_{KK}^A)^2}{2M_A} + E_{\text{el},KK}^{\text{mag}}(\mathbf{R}, \mathbf{B}) \quad (78)$$

This Berry connection term gives rise to a Berry force in addition to the bare nuclear Lorentz force.<sup>66–68</sup>

From a physically motivated point of view, a phase-space theory of coupled nuclear-electronic motion must at a minimum include such electronic screening effects; more generally, one would also expect an improved electronic structure wavefunction that accounts for the electronic motion dragged by the nuclear motion locally in an external magnetic field. Although progress on phase space electronic structure in the presence of a magnetic field is quite a bit further behind progress without such a magnetic field, we were able to construct one such approach in our recently proposed electronic phase-space Hamiltonian in an external magnetic field.<sup>34,35</sup> Our ansatz was of the form:

$$\hat{H}_{PS}(\mathbf{R}, \mathbf{P}, \mathbf{G}, \mathbf{B}) = \sum_A \frac{1}{2M_A} \left( \Pi_A^{\text{eff}} - i\hbar \hat{\Gamma}_A(\mathbf{R}) \right)^2 + \hat{H}_e(\mathbf{R}, \mathbf{G}, \mathbf{B}, \mathbf{F}) \quad (79)$$

Here, the kinetic nuclear momentum  $M\dot{\mathbf{R}} = \Pi_A^{\text{eff}} - i\hbar \hat{\Gamma}_A(\mathbf{R})$  differs from the conventional kinetic momentum  $\Pi_A$  in Eq. 78 in two ways. First, the effective nuclear momentum takes into account the static shielding of the nuclear charges experienced by the external magnetic field:

$$\Pi_A^{\text{eff}} = P_A - \frac{1}{2}q_A^{\text{eff}}(\mathbf{R})(\mathbf{B} \times (\mathbf{R}_A - \mathbf{G}_0)) \quad (80)$$

Here,  $q_A^{\text{eff}}$  is an effective nuclear charge

$$q_A^{\text{eff}}(\mathbf{R}) = Q_A e - e \langle \psi | \hat{\Theta}_A(\hat{\mathbf{r}}, \mathbf{R}) | \psi \rangle \Big|_{\mathbf{B}=0} \quad (81)$$

Second, the presence of the  $\hat{\Gamma}$  operator takes into account the electronic motion that is induced by nuclear motion, which reduces the standard PS approach as in Eq. 58 (in the absence of a magnetic field) and gives a correction to the nuclear Lorentz force similar to a Berry force (in the presence of a magnetic field).

To design a reasonable one-electron  $\hat{\Gamma}$  operator, for the most general possible approach, we must revisit the symmetry constraints in the presence of an external magnetic field. Specifically, for a charge neutral system, there are no longer six conserved quantities; instead, there are four. First, although the three components of the total canonical momentum  $\mathbf{P}_{tot} = \sum_A \mathbf{P}_A + \langle \hat{\mathbf{p}} \rangle$  are not conserved, one does conserve the three components of pseudomomentum  $\mathbf{K}_{tot} = \sum_A \mathbf{K}_A + \langle \hat{\mathbf{k}} \rangle$ . Here, we define:

$$\mathbf{K}_{A\alpha} = P_{A\alpha} + \frac{Qe}{2}(\mathbf{B} \times (\hat{\mathbf{R}}_A - \mathbf{G}_0))_\alpha \quad (82)$$

$$\hat{\mathbf{k}}_\alpha = \hat{p}_\alpha - \frac{e}{2}(\mathbf{B} \times (\hat{\mathbf{r}} - \mathbf{G}_0))_\alpha \quad (83)$$

Furthermore, the total canonical angular momentum in the direction of the external magnetic field is conserved (which is the fourth conserved quantity). Now, accounting *exactly* for these four conserved quantities is impossible within a semiclassical phase space theory because the pseudomomentum is not gauge invariant (unlike the kinetic momentum). Thus, to account approximately for the relevant conserved quantities, we have previously proposed the following constraints for  $\hat{\Gamma}$  in an external magnetic field aligned along the z-axis.<sup>34</sup>

$$-i\hbar \sum_A \hat{\Gamma}_A + \sum_A \hat{\Theta}_A \hat{\mathbf{k}}_A = 0, \quad (84)$$

$$\left[ -i\hbar \sum_B \frac{\partial}{\partial X_{B\alpha}} + \hat{p}_\alpha - i\hbar \frac{\partial}{\partial G_\alpha^0}, \hat{\Gamma}_{A\beta} \right] = 0 \quad (85)$$

$$-i\hbar \sum_A (\mathbf{R}_A - \mathbf{G}_0) \times \hat{\Gamma}_A + \sum_A \hat{\Theta}_A (\hat{\mathbf{r}} - \mathbf{G}_0) \times \hat{\mathbf{k}}_A = 0 \quad (86)$$

$$\left[ -i\hbar \sum_B \left( (\mathbf{R}_B - \mathbf{G}_0) \times \frac{\partial}{\partial \mathbf{R}_B} \right)_z + ((\hat{\mathbf{r}} - \mathbf{G}_0) \times \hat{\mathbf{p}})_z + \hat{s}_z, \hat{\Gamma}_{A\delta} \right] = i\hbar \sum_\alpha \varepsilon_{\alpha z \delta} \hat{\Gamma}_{A\alpha} \quad (87)$$

Here  $\hat{\mathbf{k}}_A$  is the electronic pseudomomentum relative to a nuclear coordinate  $\tilde{\mathbf{R}}_A$  that moves with the atoms (so that  $\hat{\mathbf{k}}_A$  is translationally invariant):

$$\hat{\mathbf{k}}_A \equiv \hat{\mathbf{k}}_e + e\mathbf{B} \times (\tilde{\mathbf{R}}_A - \mathbf{G}_0) \quad (88)$$

In Refs. 34,35 we fixed  $\tilde{\mathbf{R}}_A$  as the nuclear coordinate  $\mathbf{R}_A$ ,

$$\tilde{\mathbf{R}}_A = \mathbf{R}_A, \quad (89)$$

in order to interpret  $\hat{\mathbf{k}}_A$  as the electronic pseudomomentum partitioned locally to each nuclei. That being said, such a definition was not unique. Thus, in what follows we will also explore an alternative definition of  $\hat{\mathbf{k}}_A$  as the electronic pseudomomentum relative to a local nuclear center of charge

$$\mathbf{R}_{cc}^A = \frac{\sum_B \xi_{AB} Q_B \mathbf{R}_B}{\sum_B \xi_{AB} Q_B} \quad (90)$$

or a local center of mass

$$\mathbf{R}_{cm}^A = \frac{\sum_B \xi_{AB} M_B \mathbf{R}_B}{\sum_B \xi_{AB} M_B} \quad (91)$$

Here,  $\xi_{AB}$  is a locality function

$$\xi_{AB} = e^{-|\mathbf{R}_A - \mathbf{R}_B|^2 / \eta^2} \quad (92)$$

with a locality parameter  $\eta$ . For the calculations presented in this paper, we fixed  $\eta = \sigma$ .

If we make such a definition, in order to maintain the proper conservation laws, we must revisit the definitions of  $\Pi^{eff}$  and  $q^{eff}$  from Eqs. 80 and 81 above, and set the corresponding effective nuclear charges  $q_A^{eff}$  as:

$$\Pi_A^{eff} = \mathbf{P}_A - \frac{1}{2} q_A^{eff,cc}(\mathbf{R})(\mathbf{B} \times (\mathbf{R}_A - \mathbf{G}_0)) \quad (93)$$

$$q_A^{eff,cc}(\mathbf{R}) = Q_A e - e \sum_B \langle \Psi_0 | \hat{\Theta}_B(\hat{\mathbf{r}}, \mathbf{R}) | \Psi_0 \rangle \frac{\xi_{AB} Q_A}{\sum_C \xi_{BC} Q_C} \quad (94)$$

or

$$\Pi_A^{eff} = \mathbf{P}_A - \frac{1}{2} q_A^{eff,cm}(\mathbf{R})(\mathbf{B} \times (\mathbf{R}_A - \mathbf{G}_0)) \quad (95)$$

$$q_A^{eff,cm}(\mathbf{R}) = Q_A e - e \sum_B \langle \Psi_0 | \hat{\Theta}_B(\hat{\mathbf{r}}, \mathbf{R}) | \Psi_0 \rangle \frac{\xi_{AB} M_A}{\sum_C \xi_{BC} M_C} \quad (96)$$

In Fig. S1, we show that the local center-of-charge choice of the electronic pseudomomentum in Eq. 90 gives better results in calculating the ROA signals than fixing the pseudomomentum relative to each atom (Eq. 89). Note that, in the non-local limit  $\eta \rightarrow \infty$ ,  $\xi_{AB} \rightarrow 1$ ,  $\mathbf{R}_{cc}^A$  and  $\mathbf{R}_{cm}^A$  in Eqs. 90 and 91 become the nuclear center of charge and center of mass, respectively.

$$\hat{\mathbf{k}}_{cc}^A \equiv \hat{\mathbf{k}}_e + e\mathbf{B} \times (\mathbf{R}_{cc}^A - \mathbf{G}_0) \quad (97)$$

$$\hat{\mathbf{k}}_{cm}^A \equiv \hat{\mathbf{k}}_e + e\mathbf{B} \times (\mathbf{R}_{cm}^A - \mathbf{G}_0) \quad (98)$$

For a diatomic molecule, all of our experience suggests that the optimal choice is to fix the pseudomomentum ( $\hat{\mathbf{k}}_A$  in Eq. 88) relative to the center of mass or charge.

As shown in Ref. 34, the symmetry constraints in Eqs.84 -87 are enough to guarantee conservation of energy, the total pseudomomentum, and the total canonical angular momentum (in the  $z$ -direction). In SI section S1, we show that changing the reference frame for electronic pseudomomentum to a local nuclear center of charge or center of mass does not affect these conservation laws. To satisfy these symmetry constraints, we will construct a  $\hat{\Gamma}$  operator of the following form:<sup>34</sup>

$$\hat{\Gamma}_A = \hat{\Gamma}'_A + \hat{\Gamma}''_A \quad (99)$$

$$\hat{\Gamma}'_A = \frac{1}{2i\hbar} (\hat{\Theta}_A(\hat{\mathbf{r}})\hat{\mathbf{k}}_A + \hat{\mathbf{k}}_A\hat{\Theta}_A(\hat{\mathbf{r}})) \quad (100)$$

$$\hat{\Gamma}''_A = \sum_B \zeta_{AB} (\mathbf{R}_A - \mathbf{R}_B^0) \times \left( \mathbf{K}_B^{-1} \frac{1}{2i\hbar} (\hat{\mathbf{r}} - \mathbf{R}_B) \times (\hat{\Theta}_B(\hat{\mathbf{r}})\hat{\mathbf{k}}_B + \hat{\mathbf{k}}_B\hat{\Theta}_B(\hat{\mathbf{r}})) \right) \quad (101)$$

Here the locality functions  $\hat{\Theta}_A(\hat{\mathbf{r}})$  and  $\zeta_{AB}$  are unchanged relative to the case without the external magnetic field.

#### D. Raman Optical Activity Tensor and a Phase Space Evaluation of $W$ (Eq. 41)

It must be emphasized that, until now, the phase space theory proposed above (in Eq. 79 and Eqs. 99-101) has not been tested against experiment. Indeed, future work should certainly test such a theory against well characterized magnetic field dependent quantities, e.g. the g-factor<sup>29,69,70</sup>. That being said, the goal of this paper is to benchmark such an approach against experimental ROA data, as shown below.

To that end, let us demonstrate how to evaluate  $W$  in Eq. 41 within phase space electronic structure theory. To make progress, as noted above (Eqs. 42-43), according to BO theory and the Hamiltonian in Eq. 1, one can calculate derivatives with respect to the external magnetic field in a straightforward manner using Hellman-Feynman theorem.

$$\frac{\partial \langle \psi | \hat{H} | \psi \rangle}{\partial \mathbf{B}} = \langle \psi | \frac{\partial \hat{H}}{\partial \mathbf{B}} | \psi \rangle = - \langle \psi | \hat{\mathbf{m}} | \psi \rangle \quad (102)$$

$$\frac{\partial \langle \psi | \hat{H} | \psi \rangle}{\partial \mathbf{F}} = \langle \psi | \frac{\partial \hat{H}}{\partial \mathbf{F}} | \psi \rangle = - \langle \psi | \hat{\boldsymbol{\mu}} | \psi \rangle \quad (103)$$

By contrast, however, within an electronic phase space framework, additional derivatives must

be taken into account. Namely, note that:

$$\frac{\partial \langle \psi_{PS} | \hat{H}_{PS} | \psi_{PS} \rangle}{\partial \mathbf{B}} = \langle \psi_{PS} | \frac{\partial \hat{H}_{PS}}{\partial \mathbf{B}} | \psi_{PS} \rangle \quad (104)$$

$$\begin{aligned} &= - \langle \psi_{PS} | \hat{\mathbf{m}} | \psi_{PS} \rangle - i\hbar \frac{\mathbf{P}}{M} \cdot \left\langle \psi_{PS} \left| \frac{\partial \hat{\Gamma}}{\partial \mathbf{B}} \right| \psi_{PS} \right\rangle \\ &\quad - i\hbar \frac{\partial \Pi^{eff}}{\partial \mathbf{B}} \cdot \left\langle \psi_{PS} \left| \frac{\hat{\Gamma}}{M} \right| \psi_{PS} \right\rangle \end{aligned} \quad (105)$$

$$\frac{\partial \langle \psi_{PS} | \hat{H}_{PS} | \psi_{PS} \rangle}{\partial \mathbf{F}} = \langle \psi_{PS} | \frac{\partial \hat{H}_{PS}}{\partial \mathbf{F}} | \psi_{PS} \rangle \quad (106)$$

$$= - \langle \psi_{PS} | \hat{\boldsymbol{\mu}} | \psi_{PS} \rangle - i\hbar \frac{\mathbf{P}}{M} \cdot \left\langle \psi_{PS} \left| \frac{\partial \hat{\Gamma}}{\partial \mathbf{F}} \right| \psi_{PS} \right\rangle \quad (107)$$

where

$$\frac{\partial \Pi_{I\alpha}^{eff}}{\partial B_\beta} = -\frac{1}{2} q_I^{eff} \sum_\gamma \varepsilon_{\alpha\beta\gamma} (R_{I\gamma} - G_\gamma)$$

Re-arranging terms in Eqs. 105 and 107, we find:

$$\begin{aligned} \langle \psi_{PS} | \hat{\mathbf{m}} | \psi_{PS} \rangle &= - \frac{\partial \langle \psi_{PS} | \hat{H}_{PS} | \psi_{PS} \rangle}{\partial \mathbf{B}} - i\hbar \frac{\mathbf{P}}{M} \cdot \left\langle \psi_{PS} \left| \frac{\partial \hat{\Gamma}}{\partial \mathbf{B}} \right| \psi_{PS} \right\rangle \\ &\quad - i\hbar \frac{\partial \Pi^{eff}}{\partial \mathbf{B}} \cdot \left\langle \psi_{PS} \left| \frac{\hat{\Gamma}}{M} \right| \psi_{PS} \right\rangle \end{aligned} \quad (108)$$

$$\langle \psi_{PS} | \hat{\boldsymbol{\mu}} | \psi_{PS} \rangle = - \frac{\partial \langle \psi_{PS} | \hat{H}_{PS} | \psi_{PS} \rangle}{\partial \mathbf{F}} - i\hbar \frac{\mathbf{P}}{M} \cdot \left\langle \psi_{PS} \left| \frac{\partial \hat{\Gamma}}{\partial \mathbf{F}} \right| \psi_{PS} \right\rangle \quad (109)$$

Next we evaluate the derivatives with respect to nuclear momentum and the external fields, which are important for the ROA tensor as shown in Eq. 52.

$$\begin{aligned} \frac{\partial^2 \langle \psi_{PS} | \hat{\mathbf{m}} | \psi_{PS} \rangle}{\partial \mathbf{F} \partial \mathbf{P}} &= - \frac{\partial^3 \langle \psi_{PS} | \hat{H}_{PS} | \psi_{PS} \rangle}{\partial \mathbf{F} \partial \mathbf{P} \partial \mathbf{B}} - \frac{i\hbar}{M} \frac{\partial}{\partial \mathbf{F}} \left\langle \psi_{PS} \left| \frac{\partial \hat{\Gamma}}{\partial \mathbf{B}} \right| \psi_{PS} \right\rangle \\ &\quad - i\hbar \frac{\partial \Pi^{eff}}{\partial \mathbf{B}} \cdot \frac{\partial^2}{\partial \mathbf{F} \partial \mathbf{P}} \left\langle \psi_{PS} \left| \frac{\hat{\Gamma}}{M} \right| \psi_{PS} \right\rangle \end{aligned} \quad (110)$$

$$\frac{\partial^2 \langle \psi_{PS} | \hat{\boldsymbol{\mu}} | \psi_{PS} \rangle}{\partial \mathbf{B} \partial \mathbf{P}} = - \frac{\partial^3 \langle \psi_{PS} | \hat{H}_{PS} | \psi_{PS} \rangle}{\partial \mathbf{B} \partial \mathbf{P} \partial \mathbf{F}} - \frac{i\hbar}{M} \frac{\partial}{\partial \mathbf{B}} \left\langle \psi_{PS} \left| \frac{\partial \hat{\Gamma}}{\partial \mathbf{F}} \right| \psi_{PS} \right\rangle \quad (111)$$

Taking the difference between Eq.111 and Eq.110, the first term on the right hand side of both

equations cancel and we are left with

$$\frac{\partial W_{\gamma\alpha}}{\partial \mathbf{P}_\beta} \equiv \frac{\partial^2 \langle \psi_{PS} | \hat{\mu}_\gamma | \psi_{PS} \rangle}{\partial B_\alpha \partial \mathbf{P}_\beta} \Big|_{eq} - \frac{\partial^2 \langle \psi_{PS} | \hat{m}_\alpha | \psi_{PS} \rangle}{\partial F_\gamma \partial \mathbf{P}_\beta} \quad (112)$$

$$= -\frac{i\hbar}{M} \left( \frac{\partial}{\partial B_\alpha} \left\langle \psi_{PS} \left| \frac{\partial \hat{\Gamma}_\beta}{\partial F_\gamma} \right| \psi_{PS} \right\rangle - \frac{\partial}{\partial F_\gamma} \left\langle \psi_{PS} \left| \frac{\partial \hat{\Gamma}_\beta}{\partial B_\alpha} \right| \psi_{PS} \right\rangle \right) + i\hbar \frac{\partial \Pi^{eff}}{\partial B_\alpha} \cdot \frac{\partial^2}{\partial F_\gamma \partial \mathbf{P}_\beta} \left\langle \psi_{PS} \left| \frac{\hat{\Gamma}}{M} \right| \psi_{PS} \right\rangle \quad (113)$$

$$= \frac{i\hbar}{M} \frac{\partial}{\partial F_\gamma} \left\langle \psi_{PS} \left| \frac{\partial \hat{\Gamma}_\beta}{\partial B_\alpha} \right| \psi_{PS} \right\rangle + i\hbar \frac{\partial \Pi^{eff}}{\partial B_\alpha} \cdot \frac{\partial^2}{\partial F_\gamma \partial \mathbf{P}_\beta} \left\langle \psi_{PS} \left| \frac{\hat{\Gamma}}{M} \right| \psi_{PS} \right\rangle \quad (114)$$

As the expressions of  $\hat{\Gamma}$  in Eqs. 99-101 depend only on the external magnetic field, and not on the electric field, the first term on the right-hand-side of Eq. 114 vanishes. Note that the second term in Eq. 114 is negligible as it has a prefactor of  $M^{-2}$  whereas the first term has a prefactor of  $M^{-1}$ ; this extra factor of  $M^{-1}$  in the second term can be seen from the expression of the perturbed electronic wavefunction with respect to nuclear momentum in Eq. 32. Hence the second term in Eq. 114 is ignored for the results below, leaving the final expression:

$$\frac{\partial W_{\gamma\alpha}}{\partial \mathbf{P}_\beta} \approx \frac{i\hbar}{M} \frac{\partial}{\partial F_\gamma} \left\langle \psi_{PS} \left| \frac{\partial \hat{\Gamma}_\beta}{\partial B_\alpha} \right| \psi_{PS} \right\rangle \quad (115)$$

In the discussion section, we discuss how one might aim to include an electric-field dependence on  $\hat{\Gamma}$  as well, according to the symmetry constraints when one takes the external electric field into account. This inclusion, however, would introduce challenges that extend far beyond the scope of this paper and are left for future investigation.

Finally, a few words are appropriate with regards to computational cost. The electric-dipole magnetic-dipole polarizability  $\mathbf{G}'$  can be evaluated using Eq. 56 and Eq. 115. This phase space approach requires the calculation of only the wavefunction response to the electric field, and must be contrasted against the conventional means of evaluating  $\mathbf{G}'$  through a nuclear derivative of the Berry curvature in Eq. 19. The former is clearly much faster to evaluate than the latter because the  $\hat{\Gamma}$  and  $\frac{\partial \hat{\Gamma}_\beta}{\partial B_\alpha}$  terms in Eqs. 99-101 are one-electron operators; programmable equations are shown in the SI (Section S2).

## IV. RESULTS

We have tested the phase space approach to ROA (as established above) against experimental (R)-methyloxirane data. For these preliminary calculations, we computed optimized geometries,

Hessians and related quantities (e.g. frequencies, S-vectors) for (R)-methyloxirane within the Hartree-Fock (HF) level of theory with aug-cc-pVQZ (aQZ) basis set at the zero fields. We then computed the ROA signals, where the electric-dipole magnetic-dipole polarizabilities  $\omega^{-1}\mathbf{G}'$  were obtained with the PS approach according to Eq. 56 and with the conventional perturbation theory according to Eq. 19. In both methods, we computed the ROA tensors with aug-cc-pVTZ basis set and the gauge origin ( $\mathbf{G}_0$ ) was taken at the center of charge and the center of mass, coinciding with the coordinate origin. To calculate  $\omega^{-1}\mathbf{G}'$  with the PS approach, we evaluated the first term in 114 analytically and the second term semi-numerically. The second term was found to be negligible. All the derivatives with respect to nuclear coordinates were evaluated numerically with a step size of 0.0001 Å. To match with experimental data in Ref. 71, we used  $\omega = 488nm$  in evaluating CIDs in equations such as Eq. 27 and 57.

The calculated ROA CIDs with gauge origin ( $\mathbf{G}_0$ ) fixed at the center of charge are shown in Fig. 1. Similar results were obtained with a gauge origin fixed at the center of mass and the results are shown in Table S1. Three experimental setups from Ref. 49 are considered here: magic-angle, polarized, and depolarized measurements, presented in Fig. 1 (a), (b), and (c), respectively. The ROA CIDs calculated with the conventional perturbation approach using Eq. 27 and the phase space approach using Eq. 57 are shown in orange and blue, respectively. The experimental values reported from Ref. 71 are shown in black. We label the x-axis with the experimental vibrational frequencies and align the computed CIDs to the same frequency order observed experimentally. Admittedly, previously studies have demonstrated that frequency orders can change upon using larger basis sets and including electron-electron correlation.<sup>72</sup> To that end, for the frequency calculations, we use a large electronic basis set (aQZ) to minimize the frequency dependence on basis set choice. To investigate the effect of electron-electron correlation on the ordering of the vibrational modes, we computed vibrational frequencies with density functional theory (DFT)/B3LYP (as opposed to HF) and an aQZ basis set in Table S4. In comparing the vibrational frequencies and modes computed with HF and DFT/B3LYP, we found that the peaks at 1267  $\text{cm}^{-1}$  and 1296  $\text{cm}^{-1}$  appear in reversed order, corresponding to the experimental peaks at 1135 and 1140  $\text{cm}^{-1}$  shown in Fig. 1. As the experimental signals at these two peaks are very similar, these changes in ordering do not affect the results discussed below.

Comparing the CIDs calculated by the two approaches and also with the experimental CIDs under the three different setups in Fig. 1, we first observe that the two approaches perform similarly in terms of the number of correct signs predicted. For all three setups, the conventional BO

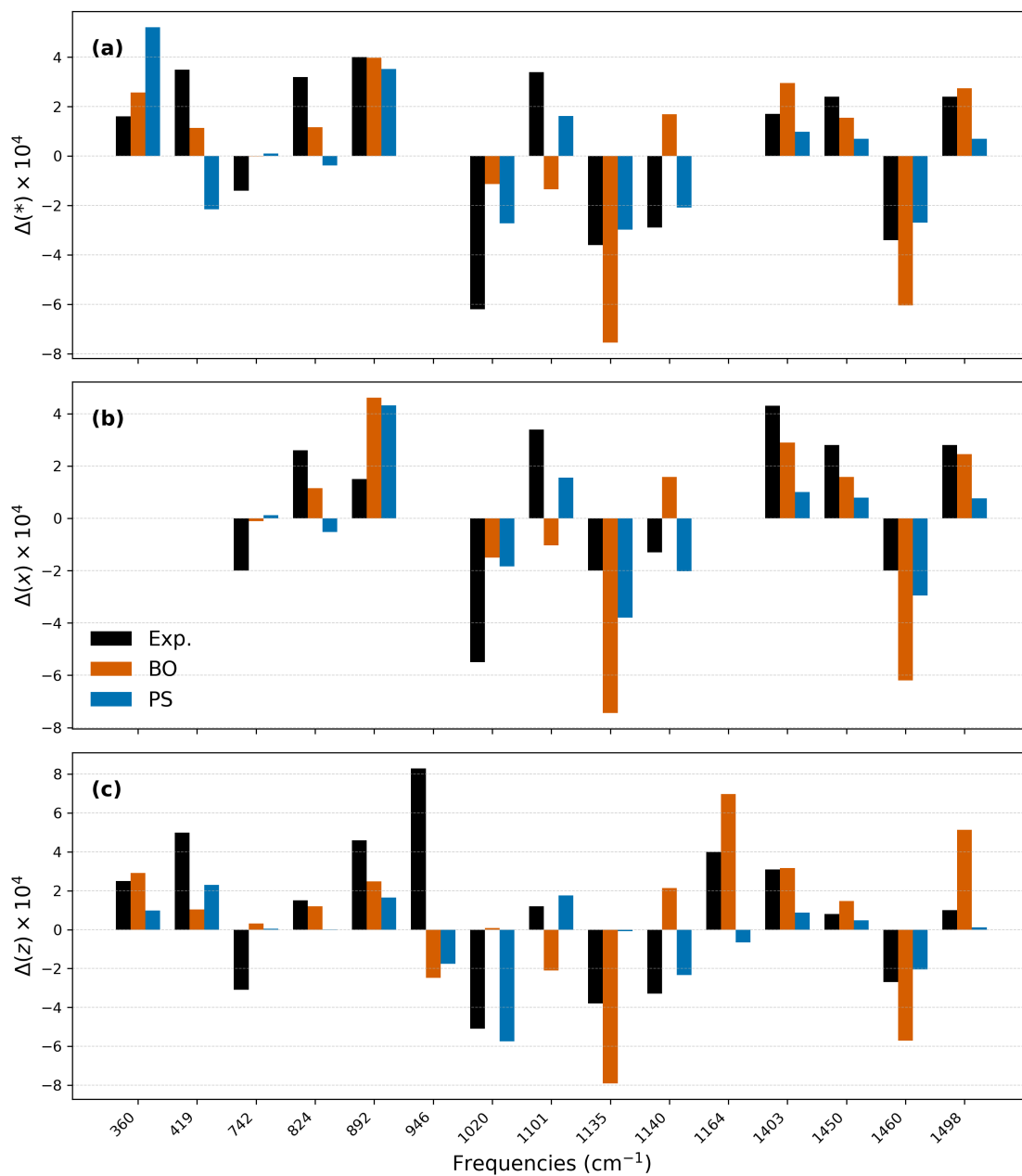


FIG. 1. Calculated (a) magic-angle ( $\Delta(*)$ ), (b) polarized ( $\Delta(x)$ ), and depolarized CIDs ( $\Delta(z)$ ) for (R)-methyloxirane using perturbation theory based on BO states (shown in orange) and PS theory (shown in blue) compared to experimental values (shown in black). The results shown here were calculated with aug-cc-pVTZ basis set. Experimental results were reported in Ref. 71. Experimentally reported frequencies were used to label x-axis.

perturbation approach predicts incorrect signs at  $1101\text{ cm}^{-1}$  and  $1140\text{ cm}^{-1}$ , which correspond to the combination of  $\text{CH}_2$  and  $\text{CH}_3$  rocking modes and the  $\text{CH}_2$  wagging mode. Similarly, the PS approach predicts incorrect signs at  $419\text{ cm}^{-1}$  and  $824\text{ cm}^{-1}$  for all three setups (except that there was no experimental data available for polarized CID at  $419\text{ cm}^{-1}$ ), which correspond to  $\text{CH}_3\text{-C}^*\text{-O}$  bending mode and a combination of  $\text{C}^*\text{-O}$  and  $\text{C-CH}_2$  stretching modes, where the asterisk (\*) indicates the chiral center. Both approaches predict a weak CID at  $742\text{ cm}^{-1}$  for all three setups, which corresponds to a combination of the  $\text{CH}_3\text{-C}^*$ ,  $\text{O-C}^*$ , and  $\text{C}^*\text{-CH}_2$  stretching modes. Second, we notice that the agreement between the computed depolarized CID results and the experimental CIDs is poorer for both computational approaches. In addition to giving CIDs with wrong signs at the previous frequencies, both approaches also predict one CID with the wrong sign at  $946\text{ cm}^{-1}$ , which corresponds to a combination of  $\text{CH}_2\text{-O}$  stretching,  $\text{C}^*\text{-CH}_3$  stretching, and  $\text{CH}_3$  rocking modes. Although the two approaches perform similarly in terms of the number of correct signs of CIDs, PS results give better root-mean-square deviation (RMSD) errors compared to experimental values for all three experimental setups, as shown in Table II. In short, the data above would appear to be rather encouraging for an initial phase space approach to ROA spectra.

	magic-angle ( $\Delta(*)$ )	polarized ( $\Delta(x)$ )	depolarized ( $\Delta(z)$ )
BO	8.23 (8.23)	10.01 (10.01)	17.89 (17.89)
PS	6.43 (6.39)	5.70 (5.65)	11.69 (11.53)

TABLE II. Root-mean-square deviation (RMSD) values relative to experimental CIDs for (R)-methyloxirane, obtained with the BO and PS approaches. The results calculated with gauge origin ( $G_0$ ) at center-of-mass is shown in the parenthesis, which are very similar to the center-of-charge results. The raw values are provided in Table S1-S3.

## V. DISCUSSION: ROBUSTNESS OF THE PS APPROACH AND ROOM FOR IMPROVEMENT

Having achieved some success in benchmarking a magnetic-field dependent PS theory, let us now further assess how robust is the algorithm and where there is room for improvement.

## A. Gauge origin sensitivity

Although the PS theory above in Eq. 79 is gauge invariant, like most magnetic field observables, a non-exact calculation of the ROA CID becomes gauge-dependent; thus, for example, when performing a calculation in an incomplete basis, the choice of origin in the magnetic dipole and electric quadrupole operators can lead to variations in the calculated intensities. The standard solutions to this is to use gauge invariant atomic orbitals (GIAOs)<sup>73,74</sup>. That being said, the results shown above in Fig. 1 and Table II use regular atomic orbitals, with gauge origin ( $\mathbf{G}_0$ ) at the center of charge, which is fixed at the origin. Although we have attempted to minimize this problem by using a large basis in Sec. IV (aug-cc-pVTZ), this problem cannot be solved without GIAOs.

To understand exactly how the problem arises, suppose one moves the gauge origin by  $\Delta$ . The changes in the effective nuclear momentum, the ETF, and the ERF components are

$$\Pi_I^{eff}(\mathbf{G}_0 + \Delta) - \Pi_I^{eff}(\mathbf{G}_0) = \frac{1}{2} q_I^{eff}(\mathbf{R})(\mathbf{B} \times \Delta) \quad (116)$$

$$\hat{\Gamma}'_I(\mathbf{G}_0 + \Delta) - \hat{\Gamma}'_I(\mathbf{G}_0) = -\frac{e}{2i\hbar} \hat{\Theta}_I(\hat{\mathbf{r}})(\mathbf{B} \times \Delta) \quad (117)$$

$$\hat{\Gamma}''_I(\mathbf{G}_0 + \Delta) - \hat{\Gamma}''_I(\mathbf{G}_0) = \sum_B \zeta_{AB} (\mathbf{R}_A - \mathbf{R}_B^0) \times \left[ \mathbf{K}_B^{-1} \left( \mathbf{J}_{\mu\nu}^B(\mathbf{G}_0 + \Delta) - \mathbf{J}_{\mu\nu}^B(\mathbf{G}_0) \right) \right] \quad (118)$$

$$J_{\mu\nu}^{B\alpha}(\mathbf{G}_0 + \Delta) - J_{\mu\nu}^{B\alpha}(\mathbf{G}_0) = -\frac{e}{2i\hbar} \sum_B (B_\alpha \Delta_\beta - B_\beta \Delta_\alpha) \langle \mu | (\hat{\mathbf{r}}_\beta - X_{B\beta}) \hat{\Theta}_B | \nu \rangle \quad (119)$$

which all go to zero when evaluated at the zero magnetic field  $\mathbf{B} = 0$ . That being said, however, the corresponding derivatives with respect to the external magnetic fields, depend on the gauge origin even at the zero magnetic field  $\mathbf{B} = 0$ .

$$\frac{\partial \Pi_{I\alpha}^{eff}(\mathbf{G}_0 + \Delta)}{\partial B_\beta} - \frac{\partial \Pi_{I\alpha}^{eff}(\mathbf{G}_0)}{\partial B_\beta} = \frac{1}{2} q_I^{eff} \sum_\gamma \varepsilon_{\alpha\beta\gamma} \Delta_\gamma \quad (120)$$

$$\frac{\partial \hat{\Gamma}'_{I\alpha}(\mathbf{G}_0 + \Delta)}{\partial B_\beta} - \frac{\partial \hat{\Gamma}'_{I\alpha}(\mathbf{G}_0)}{\partial B_\beta} = -\frac{e}{2i\hbar} \hat{\Theta}_I(\hat{\mathbf{r}}) \sum_\gamma \varepsilon_{\alpha\beta\gamma} \Delta_\gamma \quad (121)$$

$$\frac{\partial \hat{\Gamma}''_{A\alpha}(\mathbf{G}_0 + \Delta)}{\partial B_\beta} - \frac{\partial \hat{\Gamma}''_{A\alpha}(\mathbf{G}_0)}{\partial B_\beta} = \sum_B \zeta_{AB} (\mathbf{R}_A - \mathbf{R}_B^0) \times \left[ \mathbf{K}_B^{-1} \left( \frac{\partial \hat{\mathbf{J}}^B(\mathbf{G}_0 + \Delta)}{\partial B_\beta} - \frac{\partial \hat{\mathbf{J}}^B(\mathbf{G}_0)}{\partial B_\beta} \right) \right] \quad (122)$$

$$\frac{\partial \hat{\mathbf{J}}^{B\alpha}(\mathbf{G}_0 + \Delta)}{\partial B_\eta} - \frac{\partial \hat{\mathbf{J}}^{B\alpha}(\mathbf{G}_0)}{\partial B_\eta} = -\frac{e}{2i\hbar} \delta_{\alpha\eta} \sum_\kappa \Delta_\kappa (\hat{\mathbf{r}} - \mathbf{R}_B)_\kappa \hat{\Theta}_B(\hat{\mathbf{r}}) + \frac{e}{2i\hbar} \Delta_\alpha (\hat{\mathbf{r}} - \mathbf{R}_B)_\eta \hat{\Theta}_B(\hat{\mathbf{r}}) \quad (123)$$

To best understand the implications of the equations above, let us take the non-local limit  $\sigma, \beta \rightarrow \infty$ , so that  $\hat{\Theta}^A = \frac{M_A}{M_{tot}}$ , where  $M_{tot} = \sum_A M_A$ ,  $\zeta_{AB} = M_A$ ,  $\mathbf{R}_B^0 = \mathbf{R}_{CM}$ , and  $\mathbf{K}_B = I_{NCM}$ , where  $I_{NCM}$

is the nuclear moment of inertia with respect to the nuclear center of mass. Plugging the non-local limits of Eqs. 120-123 into Eq.115, and using Eq.56, one can write out the change in  $\omega^{-1}G'_{\alpha\beta}$  that arises from changing the gauge origin:

$$\begin{aligned} \omega^{-1} \left( G'_{\alpha\beta}(\mathbf{G}_0 + \Delta) - G'_{\alpha\beta}(\mathbf{G}_0) \right) = & \frac{e}{2} \left\{ \left( \frac{\sum_A M_A S_A}{M_{tot}} \times \Delta \right)_{\beta} \frac{\partial}{\partial F_{\alpha}} \langle \psi_{PS} | \psi_{PS} \rangle \right. \\ & \left. + \frac{\partial}{\partial F_{\alpha}} \left[ \left( \sum_A (\mathbf{R}_A - \mathbf{R}_{NCM}) \times \mathbf{S}_A \right) \cdot \mathbf{I}_{NCM}^{-1} \cdot \mathbf{I}_e \right]_{\beta} \right\} \langle \chi_0^{(k)} | \Pi_k | \chi_1^{(k)} \rangle \end{aligned} \quad (124)$$

where

$$I_{\eta\beta}^e = \delta_{\eta\beta} \sum_{\kappa} \Delta_{\kappa} \langle \psi_{PS} | \hat{r}_{NCM}^{\kappa} | \psi_{PS} \rangle - \Delta_{\eta} \langle \psi_{PS} | \hat{r}_{NCM}^{\beta} | \psi_{PS} \rangle \quad (125)$$

The first term on the right hand side of in Eq. 124 arises from ETFs and is exactly zero (because  $\frac{\partial}{\partial F_{\alpha}} \langle \psi_{PS} | \psi_{PS} \rangle = 0$ , i.e. the wavefunction remains normalized for all electric fields ). By contrast, the second term (that arises from the ERFs) is non-zero, as the electronic dipole moment relate to the nuclear center of mass changes with different electric fields, i.e.  $\frac{\partial}{\partial F_{\alpha}} \langle \psi_{PS} | \hat{r}_{NCM} | \psi_{PS} \rangle$  in Eq. 125 and Eq. 124 is non-zero. More generally, however, in the local limit, both ETFs and ERFs will contribute to the gauge origin dependence of the final signal and motivate the need for GIAOs.

Having analyzed the origin of the problem in theory, in Fig. 2, we next show the sensitivity of the results to the choice of gauge origin by translating the molecule 1 Å along the x, y, and z direction. In the end, we find that for some vibrations, the data is relatively robust, but for other pieces of data (especially the depolarized data), the data is still sensitive to the gauge origin. Again, in the future, we will need to implement PS ROA calculations with a GIAO basis.

## B. Momentum of the External Fields

Finally, it is worth noting that the approach above (and in Refs. 31,34) was based on the notion that we ought to build the  $\hat{\Gamma}$  operator so as to conserve the relevant momenta of the matter degrees of freedom, i.e.g without explicitly considering the momentum of the external fields. However, one can ask if one should take a further step by also considering the momentum of the external fields. Specifically, if we include the external fields, as contrasted with Eqs. 63-64 above,

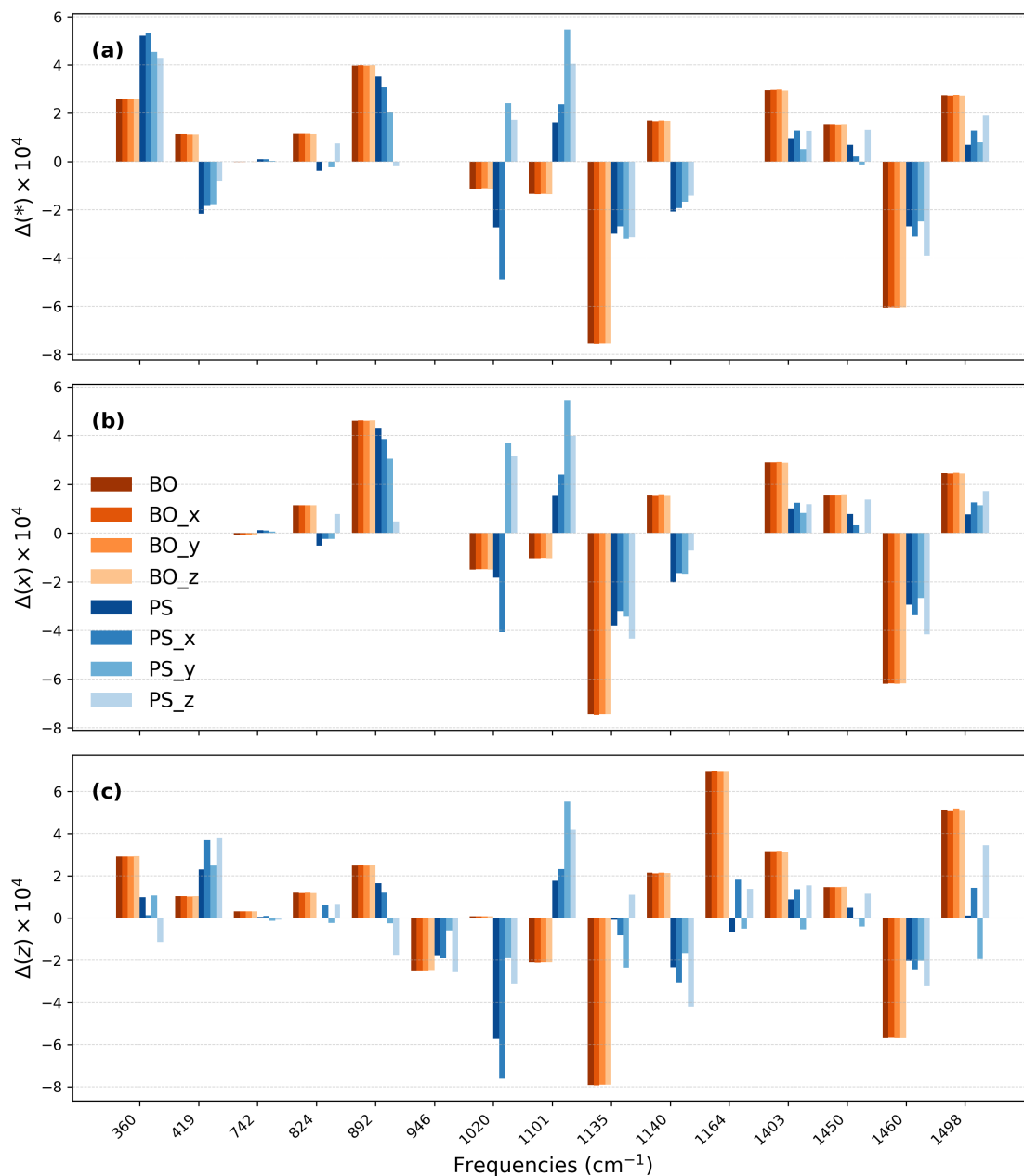


FIG. 2. Calculated (a) magic-angle ( $\Delta(*)$ ), (b) polarized ( $\Delta(x)$ ), and depolarized CIDs ( $\Delta(z)$ ) for (R)-methyloxirane using perturbation theory based on BO states (shown in orange) and PS theory (shown in blue) at different translated gauge origins. The labels with subscript x,y,z refer to translating the molecule with 1 Å along x-, y-, or z-direction. The results shown here were calculated with aug-cc-pVTZ basis set.

the natural phase conventions for the electronic states would be:

$$\left(\hat{\mathbf{P}} + \hat{\mathbf{P}}_F + \hat{\mathbf{P}}_B + \hat{\mathbf{p}}\right)\Psi(r, \mathbf{R}, \mathbf{B}, \mathbf{F}) = 0 \quad (126)$$

$$\left(\hat{\mathbf{J}} + \hat{\mathbf{J}}_F + \hat{\mathbf{J}}_B + \hat{\mathbf{j}}\right)\Psi(r, \mathbf{R}, \mathbf{B}, \mathbf{F}) = 0 \quad (127)$$

Here  $\hat{\mathbf{P}}_F = -i\hbar \frac{\partial}{\partial \mathbf{F}}$ ,  $\hat{\mathbf{P}}_B = -i\hbar \frac{\partial}{\partial \mathbf{B}}$ , and the first equation represents a phase condition for the BO wavefunction in uniform external fields for translation. Similarly  $\hat{\mathbf{J}}_F = -i\hbar \mathbf{F} \times \frac{\partial}{\partial \mathbf{F}}$ ,  $\hat{\mathbf{J}}_B = -i\hbar \mathbf{B} \times \frac{\partial}{\partial \mathbf{B}}$ , and the first equation represents a phase condition for the BO wavefunction in uniform external fields for rotation.

These conditions suggest a more general set of constraints for the  $\hat{\Gamma}$  operator

$$-i\hbar \sum_A \hat{\Gamma}_A + \hat{\mathbf{p}} - i\hbar \frac{\partial}{\partial \mathbf{F}} - i\hbar \frac{\partial}{\partial \mathbf{B}} = 0, \quad (128)$$

$$\left[-i\hbar \sum_B \frac{\partial}{\partial \mathbf{R}_B} + \hat{\mathbf{p}} - i\hbar \frac{\partial}{\partial \mathbf{F}} - i\hbar \frac{\partial}{\partial \mathbf{B}}, \hat{\Gamma}_A\right] = 0, \quad (129)$$

$$-i\hbar \sum_A \mathbf{R}_A \times \hat{\Gamma}_A + \hat{\mathbf{l}} + \hat{\mathbf{s}} - i\hbar \mathbf{F} \times \frac{\partial}{\partial \mathbf{F}} - i\hbar \mathbf{B} \times \frac{\partial}{\partial \mathbf{B}} = 0, \quad (130)$$

$$\left[-i\hbar \sum_B \left(\mathbf{R}_B \times \frac{\partial}{\partial \mathbf{R}_B}\right)_\gamma + \hat{l}_\gamma + \hat{s}_\gamma - i\hbar \mathbf{F} \times \frac{\partial}{\partial \mathbf{F}} - i\hbar \mathbf{B} \times \frac{\partial}{\partial \mathbf{B}}, \hat{\Gamma}_{A\delta}\right] = i\hbar \sum_\alpha \epsilon_{\alpha\gamma\delta} \hat{\Gamma}_{A\alpha}, \quad (131)$$

Alas, we do not know how to find solutions to such equations in any meaningful sense, but we wonder if the curious reader will have better luck than have we.

## VI. CONCLUSIONS AND FUTURE OUTLOOKS

In this paper, we have presented a new approach to the calculation of the ROA tensors from the perspective of phase electronic structure theory. Specifically, we have shown that the electric-dipole magnetic-dipole polarizability  $\mathbf{G}'$  can be viewed as the difference between changes of the electronic transition dipole moments with nuclear momentum in the presence of external electric and magnetic fields (Eq. 52), which in turn can be calculated within electronic phase space electronic structure theory (Eq.115). We have performed calculations for a prototypical molecule, methyloxirane, and found reasonable agreement with the experimental data with a reasonable choice of gauge origin.

While the results here are modestly encouraging, and the results shown here are a preliminary proof of concepts, there clearly remains a lot of work to be done to as far as practically calculating

ROA signals through the inclusion of a PS approach that includes electron-nuclear dynamic correlation. In particular, future studies will be directed to eliminate the gauge origin dependence by employing GIAOs and to investigate the form of first-order electron-nuclear correlation in the external electric fields through the  $\hat{\Gamma}$  operator. A more systematic parameterization will be important to generalize to other systems and more efficient grid evaluation will be needed to take advantage of the simple one-electron form of the  $\hat{\Gamma}$  operator.

Finally, we conclude with a few words about the Berry connection and curvature, which has plays a key role in quantum geometry, studying intriguing phenomenon such as the anomalous Hall effect<sup>75</sup> and topological insulators in materials<sup>76,77</sup> and which has recently been discussed in the context of chiral phonons<sup>78–80</sup>, which is deeply related to the CISS phenomenon<sup>81,82</sup>. The importance of Berry curvature for vibrational circular dichroism has also been pointed out in Ref. 29. Despite the many successes of the Berry curvature approach, we must emphasize that in this work, we have avoided calculating the Berry curvature. Indeed, a phase space electronic structure theory approach calculate dynamical quantities that are not available within BO theory by avoiding the BO framework entirely, and our hope is that the method can be used for a host of other applications as well, including some of the effects listed above (and more) in the future.

## VII. SUPPORTING INFORMATION

### A. Alternative Reference Frame for Electronic Pseudomomentum in Uniform Magnetic Field

In the main text of this paper, we reviewed the recently developed phase-space approach in an uniform magnetic field  $\mathbf{B}$ <sup>34,35</sup> and showed that the electron-nuclear dynamic coupling operator  $\hat{\Gamma}$  is directly related to the electronic pseudomomentum  $\hat{\mathbf{k}}_A$  relative to some nuclear coordinates  $\tilde{\mathbf{R}}_A$ .

$$\hat{\mathbf{k}}_A \equiv \hat{\mathbf{k}}_e + e\mathbf{B} \times (\tilde{\mathbf{R}}_A - \mathbf{G}) \quad (132)$$

Moreover, rather than setting

$$\tilde{\mathbf{R}}_A = \mathbf{R}_A \quad (133)$$

as we have done in the previous papers,<sup>34,35</sup> we introduced local center-of-charge  $\mathbf{R}_{cc}$  and center-of-mass  $\mathbf{R}_{cm}$  references in Eq. 90 and Eq. 91, which we repeat here, in Eqs. 134 and 135 here.

$$\mathbf{R}_{cc}^A = \frac{\sum_B \xi_{AB} Q_B \mathbf{R}_B}{\sum_B \xi_{AB} Q_B} \quad (134)$$

$$\mathbf{R}_{cm}^A = \frac{\sum_B \xi_{AB} M_B \mathbf{R}_B}{\sum_B \xi_{AB} M_B} \quad (135)$$

where  $\xi_{AB}$  is a locality function

$$\xi_{AB} = e^{-|\mathbf{R}_A - \mathbf{R}_B|^2 / \eta^2} \quad (136)$$

We will now show that this change of reference frame retains gauge invariance while conserving energy and momentum. Further, we compare the results calculated with the electronic pseudomomentum relative to each nuclei and relative to a local center-of-charge or center-of-mass.

### 1. Gauge Invariance

We know that without the  $\hat{\Gamma}$ -dependent term, the electronic BO Hamiltonian in a uniform magnetic field is gauge co-variant and the BO energy is gauge invariant. Mathematically, if

$$\hat{H}_{BO}(\mathbf{R}, \mathbf{B}, \mathbf{G})\Psi(\mathbf{r}; \mathbf{R}, \mathbf{G}) = E_{BO}(\mathbf{R}, \mathbf{B}, \mathbf{G})\Psi(\mathbf{r}; \mathbf{R}, \mathbf{G}) \quad (137)$$

then

$$\begin{aligned} \hat{H}_{BO}(\mathbf{R}, \mathbf{B}, \mathbf{G} + \Delta)\Psi(\mathbf{r}; \mathbf{R}, \mathbf{G}) \exp\left(\frac{ie}{2\hbar}(\mathbf{B} \times \Delta) \cdot \mathbf{r}\right) = \\ E_{BO}(\mathbf{R}, \mathbf{B}, \mathbf{G})\Psi(\mathbf{r}; \mathbf{R}, \mathbf{G}) \exp\left(\frac{ie}{2\hbar}(\mathbf{B} \times \Delta) \cdot \mathbf{r}\right) \end{aligned} \quad (138)$$

Now, note that changing the reference frame of the electronic pseudomomentum does not affect the gauge covariance of the  $\hat{\Gamma}$  operator because:

$$\hat{\mathbf{k}}_A(\mathbf{G}_0 + \Delta, \mathbf{B}) = \left( \hat{\mathbf{p}} - \frac{e}{2}\mathbf{B} \times (\hat{\mathbf{r}} - \mathbf{G}_0 - \Delta) + e\mathbf{B} \times (\tilde{\mathbf{R}}_A - \mathbf{G} - \Delta) \right) \quad (139)$$

$$= \left( \hat{\mathbf{p}} + \frac{e}{2}(\mathbf{B} \times \Delta) - \frac{e}{2}\mathbf{B} \times (\hat{\mathbf{r}} - \mathbf{G}_0 - \Delta) + e\mathbf{B} \times (\tilde{\mathbf{R}}_A - \mathbf{G} - \Delta) \right) \quad (140)$$

$$= \hat{\mathbf{k}}_A(\mathbf{G}_0, \mathbf{B}) \quad (141)$$

Thus, the energy remains gauge invariant.

$$\left( \frac{\partial E_{PS}}{\partial \mathbf{G}} \right)_{\Pi^{eff}} = 0 \quad (142)$$

## 2. Translational and Rotational Invariance of Energy

In Ref. 34, we have previously shown that with the  $\hat{\Gamma}$  constraints defined in Eqs. 85 and 87 (as given in Eqs. 143 and 144),

$$\left[ -i\hbar \sum_B \frac{\partial}{\partial R_{B\alpha}} + \hat{p}_\alpha - i\hbar \frac{\partial}{\partial G_\alpha^0}, \hat{\Gamma}_{A\beta} \right] = 0 \quad (143)$$

$$\left[ -i\hbar \sum_B \left( (\mathbf{R}_B - \mathbf{G}) \times \frac{\partial}{\partial \mathbf{R}_B} \right)_z + ((\hat{\mathbf{r}} - \mathbf{G}) \times \hat{\mathbf{p}})_z + \hat{s}_z, \hat{\Gamma}_{A\delta} \right] = i\hbar \sum_\alpha \varepsilon_{\alpha z \delta} \hat{\Gamma}_{A\alpha} \quad (144)$$

the total energy is translationally and rotationally invariant, i.e.,

$$\sum_A \left( \frac{\partial E_{PS}}{\partial \mathbf{R}_A} \right)_{\Pi^{eff}} + \left( \frac{\partial E_{PS}}{\partial \mathbf{G}} \right)_{\Pi^{eff}} = \sum_A \left( \frac{\partial E_{PS}}{\partial \mathbf{R}_A} \right)_{\Pi^{eff}} = 0 \quad (145)$$

$$\sum_{A\beta\gamma} \varepsilon_{z\beta\gamma} \left( P_{A\beta} \left( \frac{\partial E_{PS}}{\partial P_{A\gamma}} \right)_{\mathbf{R}} + (R_{A\beta} - G_\beta^0) \left( \frac{\partial E_{PS}}{\partial R_{A\gamma}} \right)_{\mathbf{P}} \right) = 0 \quad (146)$$

The local center of charge or mass in Eq. 134 or 135 only depends on nuclear coordinates (just like the choice of Eq. 133 previously). Furthermore, translating all the nuclei shifts the reference frame same as before.

$$\sum_B \frac{\partial \mathbf{R}_{cc}^A}{\partial \mathbf{R}_B} = \sum_B \frac{\partial \mathbf{R}_{cc}^A}{\partial \xi_{AB}} \frac{\partial \xi_{AB}}{\partial \mathbf{R}_B} + \sum_B \delta_{BC} \frac{\sum_C \xi_{AC} Q_C}{\sum_C \xi_{AC} Q_C} = 1 = \sum_B \frac{\partial \mathbf{R}^A}{\partial \mathbf{R}_B} \quad (147)$$

The term involves  $\frac{\partial \xi_{AB}}{\partial \mathbf{R}_B}$  in Eq. 147 goes to zero, because the locality function  $\xi_{AB}$  depends on the relative distance between  $\mathbf{R}_A$  and  $\mathbf{R}_B$ , and hence does not change with translation and rotation. Therefore the new reference frame still satisfies the same constraint in Eqs. 85 as before and hence conserves the total energy under translation. A similar statement holds for conservation under rotation.

## 3. Momentum Conservation

In this section, we write down the expression for the  $q^{eff}$  with the new reference frame for the electronic pseudomomentum for the choice of local center of charge  $\tilde{\mathbf{R}}_A = \mathbf{R}_{cc}^A$  in Eq. 134 and the corresponding conserved linear and angular momentum. We start with the phase-space energy in a uniform magnetic field  $\mathbf{B}$ :

$$E_{PS}(\mathbf{R}, \mathbf{P}, \mathbf{B}) = \sum_A \frac{(\Pi_A^{eff})^2}{2M_A} + V_{PS}(\mathbf{R}, \mathbf{P}, \mathbf{B}) \quad (148)$$

$$V_{PS}(\mathbf{R}, \mathbf{P}, \mathbf{B}) = \sum_i \frac{\langle \pi_i^2 \rangle}{2} + \langle V_{eN} \rangle + \langle V_{ee} \rangle - i\hbar \sum_A \frac{\Pi_A^{eff} \cdot \langle \hat{\Gamma}_A \rangle}{M_A} - \hbar^2 \sum_A \frac{\langle \hat{\Gamma}_A^2 \rangle}{2M_A} \quad (149)$$

where  $V_{PS}$  is obtained by diagonalizing the electronic phase space Hamiltonian in an external magnetic field. The nuclear kinetic momentum with effective nuclear charges is defined as:

$$\mathbf{\Pi}_A^{eff} = \mathbf{P}_A - \frac{1}{2}q_A^{eff}(\mathbf{R})(\mathbf{B} \times (\mathbf{R}_A - \mathbf{G})) \quad (150)$$

Note that here (and above and below), we always assume that  $q_A^{eff}(\mathbf{R})$  does not depend on  $B$ . To find an expression for the nuclear pseudomomentum, we start with a phase space equation of motion for the nuclear kinetic momentum:

$$\mathbf{\Pi}_{A\alpha}^{kin,eff} = M_A \dot{R}_{A\alpha} = \left( \frac{\partial E_{PS}}{\partial P_{A\alpha}} \right)_X = \mathbf{\Pi}_{A\alpha}^{eff} - i\hbar \langle \psi_{PS} | \hat{\Gamma}_{A\alpha} | \psi_{PS} \rangle \quad (151)$$

This expression for the effective kinetic momentum  $\mathbf{\Pi}^{kin,eff}$  can be used to write the nuclear pseudomomentum  $\mathbf{K}_{eff}$  as follows:

$$\mathbf{K}_{eff}^\alpha \equiv \sum_A \mathbf{\Pi}_{A\alpha}^{kin,eff} + \sum_A q_A^{eff}(\mathbf{R})(\mathbf{B} \times (\mathbf{R}_A - \mathbf{G}_0))_\alpha \quad (152)$$

$$= \sum_A P_{A\alpha} + \frac{1}{2} \sum_A q_A^{eff}(\mathbf{R})(\mathbf{B} \times (\mathbf{R}_A - \mathbf{G}_0))_\alpha - i\hbar \langle \psi_{PS} | \hat{\Gamma}_{A\alpha} | \psi_{PS} \rangle \quad (153)$$

where the  $q_A^{eff}$  is defined as (following Eq. 94):

$$q_A^{eff,cc}(\mathbf{R}) = Q_A e - e \sum_B \langle \Psi_0 | \hat{\Theta}_B(\hat{\mathbf{r}}, \mathbf{R}) | \Psi_0 \rangle \frac{\zeta_{AB} Q_A}{\sum_C \zeta_{BC} Q_C} \quad (154)$$

Here, the  $\hat{\Theta}_B$  term partitions the space around each nuclei in such a way that the electrons in that region would also be translated or rotated with the nuclei. The  $\zeta_{BA}$  factor defines the pseudomomentum of electrons with respect to a localized nuclear center-of-charge around each of the atoms. The end result is a  $\Gamma$  term that is translationally invariant (which would not be possible using the standard pseudomomentum). Note that Eq. 153. can be rearranged as follows:

$$\mathbf{K}_{eff}^\alpha = \sum_A P_{A\alpha} - \frac{1}{2} \sum_A q_A^{eff}(\mathbf{R})(\mathbf{B} \times (\mathbf{R}_A - \mathbf{G}_0))_\alpha - i\hbar \langle \psi_{PS} | \hat{\Gamma}_{A\alpha} | \psi_{PS} \rangle + \sum_A q_A^{eff}(\mathbf{R})(\mathbf{B} \times (\mathbf{R}_A - \mathbf{G}_0))_\alpha \quad (155)$$

$$= \sum_A \mathbf{\Pi}_{A\alpha}^{kin,eff} + \sum_A q_A^{eff}(\mathbf{R})(\mathbf{B} \times (\mathbf{R}_A - \mathbf{G}_0))_\alpha \quad (156)$$

$$= \sum_A \mathbf{\Pi}_{A\alpha}^{kin,eff} + Q_A e (\mathbf{B} \times (\mathbf{R}_A - \mathbf{G}_0))_\alpha - \tilde{D}_{\mu\nu} \sum_B \Theta_B \left( \frac{\zeta_{BA} Q_A (\mathbf{B} \times (\mathbf{R}_A - \mathbf{G}_0))_\alpha}{\sum_C \zeta_{BC} Q_B} \right) \quad (157)$$

where the phase space kinetic momentum is defined in Eq. 151 and we have plugged in the definition of  $q^{eff}$  in Eq. 154. Next, we posit an electronic pseudomomentum of the form:

$$\langle k_e^\alpha \rangle \equiv \sum_A \langle k^{A\alpha} \rangle \quad (158)$$

$$= \langle k^\alpha \rangle + \sum_A \langle \Theta_A \rangle \frac{\sum_B \zeta_{AB} Q_B (\mathbf{B} \times (\mathbf{R}_B - \mathbf{G}))_\alpha}{\sum_B \zeta_{AB} Q_B} \quad (159)$$

With these definitions, for a collection of nuclei with charges  $q_A^{eff}$  and electrons with charge  $-e$  (we define  $e > 0$ ), we further posit a total pseudomomentum of the form:

$$\mathbf{K}_{mol}^\alpha \equiv \mathbf{K}_{eff}^\alpha + \langle \mathbf{k}_e^\alpha \rangle \quad (160)$$

If we add Eq. 157 and Eq. 159 and notice that the extra term in Eq. 159 (arising from the choice of reference for pseudomomentum) cancels with the extra term in Eq. 157 (arising from the corresponding change to the nuclear effective charge), it follows that

$$\mathbf{K}_{mol}^\alpha = \sum_A \left( \Pi_{A\alpha}^{kin,eff} + Q_A e (\mathbf{B} \times (\mathbf{R}_A - \mathbf{G}))_\alpha \right) + \langle \hat{k}_\alpha \rangle \quad (161)$$

Note that Eq. 161 which is the sum of the pseudomomenta of effective nuclear charges ( $\mathbf{K}_A^{eff}$ ) and the effective pseudomomenta of electrons ( $\hat{\mathbf{k}}$ ) is conserved by phase space dynamics. Ref. 34 shows clearly that  $\mathbf{K}_{mol}$  in Eq. 161 is conserved. This approach makes clear that we must choose the choice of effective charge (in Eq. 154) to match the pseudomomentum reference center (in Eq. 132). Likewise it can also be shown that the total angular momentum is conserved in the direction of the magnetic field. For a given magnetic field in the z-direction, the total conserved angular momentum is<sup>34</sup>

$$L_{mol}^z = L_z + \langle \hat{l}_z \rangle \quad (162)$$

$$L_z = \sum_A \left( (\mathbf{R}_A - \mathbf{G}) \times \left( \Pi_A^{kin,eff} + \frac{q_A^{eff}(\mathbf{R})}{2} (\mathbf{B} \times (\mathbf{R}_A - \mathbf{G})) \right) \right)_z \quad (163)$$

$$\langle \hat{l}_z \rangle = \sum_A \left\langle \psi_{PS} \left| \left( (\hat{\mathbf{r}} - \mathbf{G}) \times \hat{\Theta}_A \hat{\mathbf{k}}_A \right)_z \right| \psi_{PS} \right\rangle \quad (164)$$

#### 4. ROA Circular Intensity Difference

In Fig. 3, we compare the ROA circular intensity differences (CID) calculated with different reference frames for the electronic pseudomomentum to the experimental values reported in Ref. 71. The best agreement with experimental CIDs (shown in black) was found with the calculation of the electronic pseudomomentum relative to a local center of charge (shown in blue), which is also the data shown in Fig. 1 in the main paper. If the non-local limit was adopted using either the total center-of-charge (shown in green) or the total center-of-mass (shown in yellow), the agreement with experiment becomes worse, suggesting the importance of locality. The previous choice of calculating the electronic pseudomomentum relative to the nuclear coordinates (shown in orange)

does not give as good match with experimental CIDs as the local center of charge, suggesting the need for some delocalization and smooth switching function.

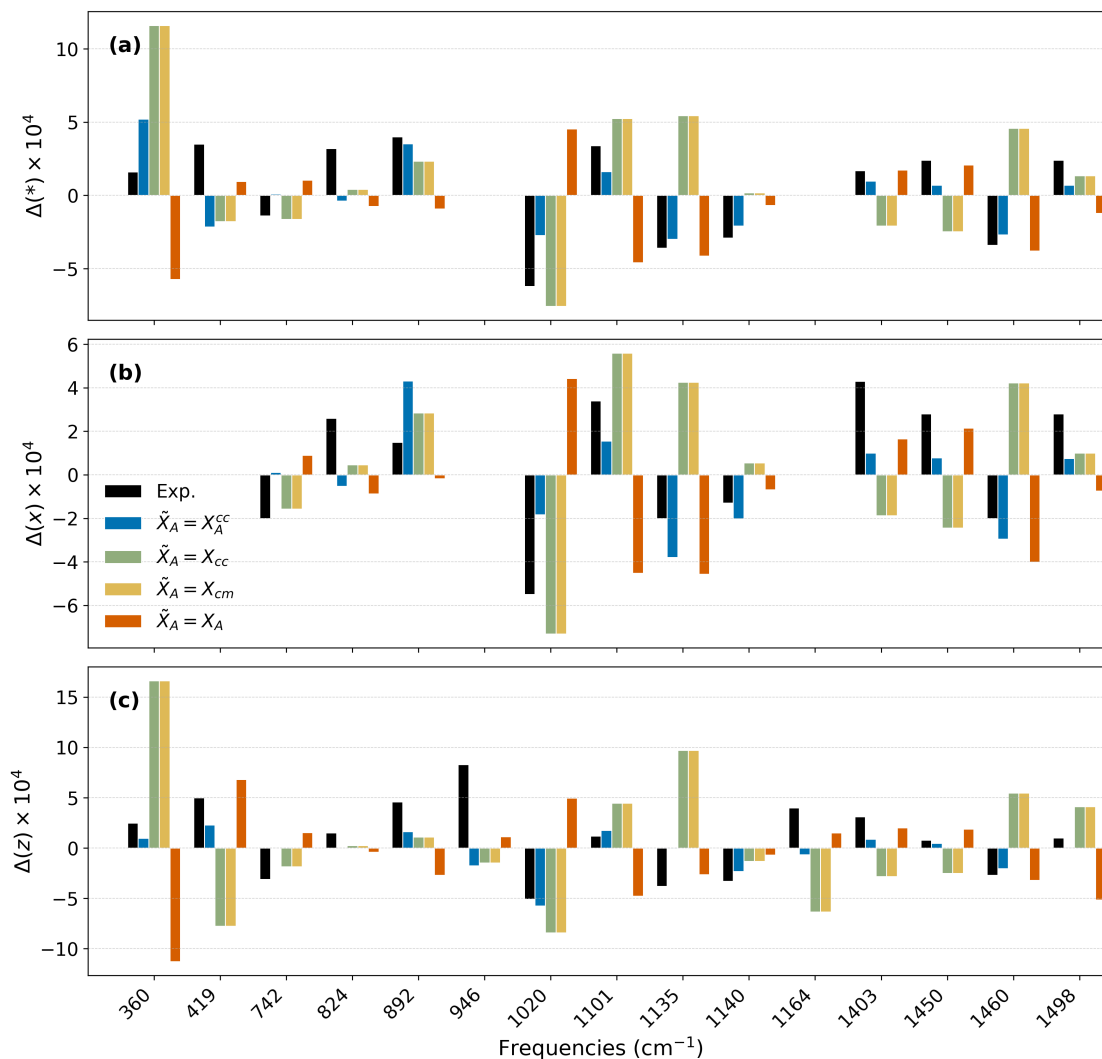


FIG. 3. Calculated (a) magic-angle ( $\Delta(*)$ ), (b) polarized ( $\Delta(x)$ ), and depolarized CIDs ( $\Delta(z)$ ) for (R)-methyloxirane using different reference frames for electronic pseudomomentum in the PS theory compared to experimental values (shown in black). See text for the definitions of the curves with other colors. The results shown here were calculated with aug-cc-pVTZ basis set. Experimental results were reported in Ref. 71. Experimentally reported frequencies were used to label x-axis. This data makes clear that some locality (but not strict locality) is best for establishing a reference frame.

## B. Programmable equations for Gamma derivatives

In this section, we provide the programmable equations for the atomic orbital (AO) matrix elements for the  $\hat{\Gamma}$  operator  $\langle \mu | \hat{\Gamma} | \nu \rangle$  and  $\left\langle \mu \left| \frac{\partial \hat{\Gamma}_\beta}{\partial B_\alpha} \right| \nu \right\rangle$  in a uniform external magnetic field, . The matrix elements for  $\hat{\Gamma}$  operator  $\langle \mu | \hat{\Gamma} | \nu \rangle$  consists of a translational coupling component and a rotational coupling component:

$$\langle \mu | \hat{\Gamma} | \nu \rangle = \langle \mu | \hat{\Gamma}' | \nu \rangle + \langle \mu | \hat{\Gamma}'' | \nu \rangle \quad (165)$$

where

$$\hat{\Gamma}'_A = \frac{1}{2i\hbar} (\hat{\Theta}_A(\hat{r}) \hat{k}_A + \hat{k}_A \hat{\Theta}_A(\hat{r})) \quad (166)$$

and

$$\hat{\Gamma}''_A = \sum_B \zeta_{AB} (\mathbf{R}_A - \mathbf{R}_B^0) \times \left( \mathbf{K}_B^{-1} \frac{1}{2i\hbar} (\hat{r} - \mathbf{R}_B) \times (\hat{\Theta}_B(\hat{r}) \hat{k}_B + \hat{k}_B \hat{\Theta}_B(\hat{r})) \right) \quad (167)$$

Recall the definition for  $\hat{k}_A$ ,

$$\hat{k}_A \equiv \hat{k}_e + e\mathbf{B} \times (\tilde{\mathbf{R}}_A - \mathbf{G}) \quad (168)$$

$$= \hat{p} - \frac{e}{2} (\mathbf{B} \times (\hat{r} - \mathbf{G})) + e\mathbf{B} \times (\tilde{\mathbf{R}}_A - \mathbf{G}) \quad (169)$$

Plugging in the definition of  $\hat{k}_A$  into Eq. 166, the AO matrix elements for  $\hat{\Gamma}'$  are

$$\begin{aligned} -i\hbar \langle \mu | \hat{\Gamma}'_{A\beta} | \nu \rangle &= \frac{i\hbar}{2} \left( \langle \mu | \hat{\Theta}_A | \nabla_\beta \nu \rangle - \langle \nabla_\beta \mu | \hat{\Theta}_A | \nu \rangle \right) \\ &+ \frac{e}{2} \left\langle \mu \left| \left[ \mathbf{B} \times (\hat{r} - 2\tilde{\mathbf{R}}_A + \mathbf{G}_0) \right]_\beta \hat{\Theta}_A \right| \nu \right\rangle \end{aligned} \quad (170)$$

The AO matrix elements for  $\hat{\Gamma}''$  are

$$-i\hbar \langle \mu | \hat{\Gamma}''_A | \nu \rangle = -i\hbar \sum_B \zeta_{AB} (\mathbf{R}_A - \mathbf{R}_B^0) \times \left( \mathbf{K}_B^{-1} J_{\mu\nu}^B \right) \quad (171)$$

Here  $\zeta_{AB}$  is a locality function, where  $\zeta_{AB} = M_A e^{-|\mathbf{R}_A - \mathbf{R}_B|^2 / \beta_{AB}^2}$ .  $\mathbf{K}_B$  is a moment-of-inertial like tensor, where  $\mathbf{K}_B = -\sum_A \zeta_{AB} ((\mathbf{R}_A - \mathbf{R}_B^0) \mathbf{R}_A^\top - \mathbf{R}_A^\top (\mathbf{R}_A - \mathbf{R}_B^0) \mathcal{I}_3)$ .  $\mathbf{R}_B^0$  is an averaged position,

$\mathbf{R}_B^0 = \frac{\sum_A \zeta_{AB} \mathbf{R}_A}{\sum_A \zeta_{AB}}$ , and  $\mathcal{I}_3$  is a 3 by 3 identity matrix. The expression for matrix elements for  $J_{\mu\nu}^B$  is

$$-i\hbar J_{\mu\nu}^{B\alpha} = \sum_{\beta\gamma} \varepsilon_{\alpha\beta\gamma} \left( \frac{i\hbar}{2} \left[ \langle \mu | (\hat{\mathbf{r}} - \mathbf{R}_B)_\beta \hat{\Theta}_B | \nabla_\gamma \mathbf{v} \rangle - \langle \nabla_\gamma \mu | (\hat{\mathbf{r}} - \mathbf{R}_B)_\beta \hat{\Theta}_B | \mathbf{v} \rangle \right] \right. \\ \left. + \frac{e}{2} \sum_{\eta\kappa} \varepsilon_{\gamma\eta\kappa} \langle \mu | (\hat{\mathbf{r}} - \mathbf{R}_B)_\beta B_\eta (\hat{\mathbf{r}} - 2\tilde{\mathbf{R}}_B + \mathbf{G}_0)_\kappa \hat{\Theta}_B | \mathbf{v} \rangle \right) \quad (172)$$

$$= \frac{i\hbar}{2} \sum_{\beta\gamma} \varepsilon_{\alpha\beta\gamma} \left( \langle \mu | (\hat{\mathbf{r}} - \mathbf{R}_B)_\beta \hat{\Theta}_B | \nabla_\gamma \mathbf{v} \rangle - \langle \nabla_\gamma \mu | (\hat{\mathbf{r}} - \mathbf{R}_B)_\beta \hat{\Theta}_B | \mathbf{v} \rangle \right) \\ + \frac{e}{2} \sum_{\beta} \langle \mu | (\hat{\mathbf{r}} - \mathbf{R}_B)_\beta B_\alpha (\hat{\mathbf{r}} - 2\tilde{\mathbf{R}}_B + \mathbf{G}_0)_\beta \hat{\Theta}_B | \mathbf{v} \rangle \\ - \frac{e}{2} \sum_{\beta} \langle \mu | (\hat{\mathbf{r}} - \mathbf{R}_B)_\beta B_\beta (\hat{\mathbf{r}} - 2\tilde{\mathbf{R}}_B + \mathbf{G}_0)_\alpha \hat{\Theta}_B | \mathbf{v} \rangle \quad (173)$$

$$= \frac{i\hbar}{2} \sum_{\beta\gamma} \varepsilon_{\alpha\beta\gamma} \left( \langle \mu | (\hat{\mathbf{r}} - \mathbf{R}_B)_\beta \hat{\Theta}_B | \nabla_\gamma \mathbf{v} \rangle - \langle \nabla_\gamma \mu | (\hat{\mathbf{r}} - \mathbf{R}_B)_\beta \hat{\Theta}_B | \mathbf{v} \rangle \right) \\ + \frac{e}{2} \sum_{\beta} B_\alpha \left( \langle \mu | \hat{r}_\beta^2 \hat{\Theta}_B | \mathbf{v} \rangle + (G_\beta - X_{B\beta} - 2\tilde{R}_{B\beta}) \langle \mu | \hat{r}_\beta \hat{\Theta}_B | \mathbf{v} \rangle - X_{B\beta} (G_\beta - 2\tilde{R}_{B\beta}) \langle \mu | \hat{\Theta}_B | \mathbf{v} \rangle \right) \\ - \frac{e}{2} \sum_{\beta} B_\beta \left[ \langle \mu | \hat{r}_\beta \hat{r}_\alpha \hat{\Theta}_B | \mathbf{v} \rangle + (G_\alpha - 2\tilde{R}_{B\alpha}) \langle \mu | \hat{r}_\beta \hat{\Theta}_B | \mathbf{v} \rangle - X_{B\beta} \langle \mu | \hat{r}_\alpha \hat{\Theta}_B | \mathbf{v} \rangle \right. \\ \left. - X_{B\beta} (G_\alpha - 2\tilde{R}_{B\alpha}) \langle \mu | \hat{\Theta}_B | \mathbf{v} \rangle \right] \quad (174)$$

Here, to go from Eq. 172 to Eq. 173, we evaluated the product of the Levi-Civita symbols,

$$\sum_{\gamma} \varepsilon_{\alpha\beta\gamma} \varepsilon_{\gamma\kappa\eta} = \delta_{\alpha\kappa} \delta_{\beta\eta} - \delta_{\alpha\eta} \delta_{\beta\kappa} \quad (175)$$

Now we present the programmable equations for  $\left\langle \mu \left| \frac{\partial \hat{\Gamma}_\beta}{\partial B_\alpha} \right| \mathbf{v} \right\rangle$ . We first evaluate

$$\frac{\partial \hat{k}_{A\alpha}}{\partial B_\beta} = -\frac{e}{2} \sum_{\gamma} \varepsilon_{\alpha\beta\gamma} (\hat{\mathbf{r}} - \mathbf{G})_\gamma + e \sum_{\gamma} \varepsilon_{\alpha\beta\gamma} (\mathbf{R}_A - \mathbf{G})_\gamma \quad (176)$$

$$= -\frac{e}{2} \sum_{\gamma} \varepsilon_{\alpha\beta\gamma} \hat{r}_\gamma - \frac{e}{2} \sum_{\gamma} \varepsilon_{\alpha\beta\gamma} G_\gamma + e \sum_{\gamma} \varepsilon_{\alpha\beta\gamma} R_{A\gamma} \quad (177)$$

Taking derivative of  $\left\langle \mu \left| \hat{\Gamma}'_{A\beta} \right| \mathbf{v} \right\rangle$  in Eq. 170 with respect to the external magnetic field at  $\mathbf{B} = 0$ , we get

$$\frac{\partial \hat{\Gamma}'_{A\alpha}}{\partial B_\beta} = \frac{1}{i\hbar} \hat{\Theta}_A(\hat{\mathbf{r}}) \frac{\partial \hat{k}_{A\alpha}}{\partial B_\beta} \quad (178)$$

$$-i\hbar \frac{\partial \langle \mu | \hat{\Gamma}'_{A\alpha} | \mathbf{v} \rangle}{\partial B_\beta} = \frac{e}{2} \sum_{\gamma} \varepsilon_{\alpha\beta\gamma} \left( \langle \mu | \hat{r}_\gamma \hat{\Theta}_A(\hat{\mathbf{r}}) | \mathbf{v} \rangle + (G_\gamma - 2R_{A\gamma}) \langle \mu | \hat{\Theta}_A(\hat{\mathbf{r}}) | \mathbf{v} \rangle \right) \quad (179)$$

Similarly, taking the derivative of  $\langle \mu | \hat{\Gamma}_{AB}'' | \nu \rangle$  in Eq. 174 with respect to the external magnetic field at  $\mathbf{B} = 0$ , we find

$$-i\hbar \langle \mu | \frac{\partial \hat{\Gamma}_A''}{\partial \mathbf{B}} | \nu \rangle = -i\hbar \sum_B \zeta_{AB} (\mathbf{R}_A - \mathbf{R}_B^0) \times \left( \mathbf{K}_J^{-1} (\hat{\mathbf{r}} - \mathbf{R}_B) \times \frac{\partial \hat{\Gamma}'}{\partial \mathbf{B}} \right) \quad (180)$$

$$= -i\hbar \sum_B \zeta_{AB} (\mathbf{R}_A - \mathbf{R}_B^0) \times \left( \mathbf{K}_B^{-1} \frac{\partial \hat{\mathbf{J}}_{\mu\nu}^B}{\partial \mathbf{B}} \right) \quad (181)$$

$$-i\hbar \frac{\partial J_{\mu\nu}^{B\alpha}}{\partial B_\eta} = \frac{e}{2} \sum_{\beta\gamma\kappa} \varepsilon_{\alpha\beta\gamma} \varepsilon_{\gamma\eta\kappa} \left( \left[ \langle \mu | (\hat{\mathbf{r}} - \mathbf{R}_B)_\beta \hat{r}_\kappa \hat{\Theta}_B | \nu \rangle + (G_\kappa - 2R_{B\kappa}) \langle \mu | (\hat{\mathbf{r}} - \mathbf{R}_B)_\beta \hat{\Theta}_B(\hat{\mathbf{r}}) | \nu \rangle \right] \right) \quad (182)$$

$$= \frac{e}{2} \delta_{\alpha\eta} \left( \sum_\kappa \langle \mu | (\hat{\mathbf{r}} - \mathbf{R}_B)_\kappa \hat{r}_\kappa \hat{\Theta}_B | \nu \rangle + (G_\kappa - 2R_{B\kappa}) \langle \mu | (\hat{\mathbf{r}} - \mathbf{R}_B)_\kappa \hat{\Theta}_B(\hat{\mathbf{r}}) | \nu \rangle \right) \\ - \frac{e}{2} \left( \left[ \langle \mu | (\hat{\mathbf{r}} - \mathbf{R}_B)_\eta \hat{r}_\alpha \hat{\Theta}_B | \nu \rangle + (G_\alpha - 2R_{B\alpha}) \langle \mu | (\hat{\mathbf{r}} - \mathbf{R}_B)_\eta \hat{\Theta}_B(\hat{\mathbf{r}}) | \nu \rangle \right] \right) \quad (183)$$

### C. ROA Circular Intensity Difference

In Tables III- V we report all the raw data for Fig. 1 in the main paper, where the nuclear center of charge is placed at the origin of the coordinate system. We denote these data by the subscript "coc". In addition, we also show the CIDs with the nuclear center of mass placed at the origin of the coordinate system, denoted by the subscript "com". The nuclear center of mass and the center of charge differ by 0.1 Bohr. Neither the BO nor PS results are very sensitive to this small change of the origin ( $G_0$ ). Note that all the data in Tables III-V below use the local center of charge reference frame  $\tilde{\mathbf{R}}_A = \mathbf{R}_{cc}^A$  to define the electronic pseudomomentum in Eq. 132.

TABLE III. Magic-angle CID computed with both the conventional perturbation approach and the phase space approach as calculated at different gauge origins ( $G_0$ ).

Vib. Freq. ( $\text{cm}^{-1}$ )		Magic-angle CID				
Hartree-Fock	Exp.	Exp.	BO_com	PS_com	BO_coc	PS_coc
227	200		2.53	-17.89	2.53	-17.42
397	360	1.6	2.58	5.2	2.58	5.21
442	419	3.5	1.14	-2.14	1.14	-2.16
851	742	-1.4	-0.02	0.1	-0.02	0.1
940	824	3.2	1.16	-0.37	1.16	-0.39
986	892	4	3.98	3.46	3.98	3.52
1070	946		-1.44	-0.7	-1.44	-0.72
1139	1020	-6.2	-1.13	-2.67	-1.13	-2.73
1238	1101	3.4	-1.35	1.79	-1.35	1.62
1267	1135	-3.6	-7.55	-2.98	-7.55	-2.99
1296	1140	-2.9	1.69	-2.06	1.69	-2.08
1310	1164		4.11	0.01	4.11	0.08
1407	1262		-0.46	0.36	-0.46	0.38
1526	1365		-1.23	2.54	-1.23	2.34
1574	1403	1.7	2.96	0.97	2.96	0.98
1600	1450	2.4	1.55	0.64	1.55	0.7
1614	1460	-3.4	-6.05	-2.7	-6.05	-2.69
1672	1498	2.4	2.75	0.72	2.75	0.69
3162			0.06	0.01	0.06	0.01
3217			-0.003	0.05	-0.003	0.04
3231			-1.41	-0.13	-1.41	-0.12
3242			0.57	0.07	0.57	0.08
3261			1.01	0.01	1.01	0
3324			-0.72	0.02	-0.72	0.02

TABLE IV. Polarized CID computed with both the conventional perturbation approach and the phase space approach as calculated at different gauge origins ( $G_0$ ).

Vib. Freq. ( $\text{cm}^{-1}$ )		Polarized CID				
Hartree-Fock	Exp.	Exp.	BO_com	PS_com	BO_coc	PS_coc
227	200		1.92	-29.96	1.92	-29.33
397	360		2.46	6.62	2.47	6.63
442	419		1.16	-2.91	1.16	-2.93
851	742	-2	-0.11	0.12	-0.11	0.12
940	824	2.6	1.15	-0.51	1.15	-0.53
986	892	1.5	4.61	4.27	4.61	4.32
1070	946		-1.25	-0.51	-1.25	-0.53
1139	1020	-5.5	-1.5	-1.76	-1.5	-1.83
1238	1101	3.4	-1.03	1.73	-1.03	1.56
1267	1135	-2	-7.44	-3.75	-7.44	-3.8
1296	1140	-1.3	1.58	-1.99	1.58	-2.02
1310	1164		3.54	0.12	3.54	0.23
1407	1262		-0.37	0.29	-0.37	0.31
1526	1365		-1.11	2.12	-1.11	1.93
1574	1403	4.3	2.9	1.01	2.9	1.01
1600	1450	2.8	1.58	0.73	1.58	0.79
1614	1460	-2	-6.19	-2.96	-6.19	-2.95
1672	1498	2.8	2.45	0.8	2.45	0.76
3162			0.05	0.01	0.05	0.01
3217			0.03	0.1	0.03	0.09
3231			-1.51	-0.25	-1.51	-0.24
3242			0.5	0.18	0.5	0.18
3261			0.85	-0.01	0.85	-0.02
3324			-0.83	-0.06	-0.83	-0.06

TABLE V. Depolarized CID computed with both the conventional perturbation approach and the phase space approach at different gauge origins ( $G_0$ )

Vib. Freq. ( $\text{cm}^{-1}$ )		Depolarized CID				
Hartree-Fock	Exp.	Exp.	BO_com	PS_com	BO_coc	PS_coc
227	200		4.08	12.97	4.08	13.04
397	360	2.5	2.92	0.96	2.92	0.99
442	419	5	1.04	2.36	1.04	2.29
851	742	-3.1	0.32	0.04	0.32	0.04
940	824	1.5	1.2	0.001	1.2	-0.02
986	892	4.6	2.49	1.57	2.49	1.65
1070	946	8.3	-2.48	-1.72	-2.49	-1.76
1139	1020	-5.1	0.08	-5.7	0.08	-5.74
1238	1101	1.2	-2.11	1.92	-2.11	1.77
1267	1135	-3.8	-7.92	-0.21	-7.92	-0.08
1296	1140	-3.3	2.15	-2.34	2.15	-2.34
1310	1164	4	6.97	-0.55	6.97	-0.66
1407	1262		-0.95	0.77	-0.95	0.75
1526	1365		-1.8	4.56	-1.8	4.31
1574	1403	3.1	3.16	0.84	3.16	0.88
1600	1450	0.8	1.47	0.43	1.47	0.49
1614	1460	-2.7	-5.7	-2.06	-5.7	-2.04
1672	1498	1	5.14	0.08	5.14	0.11
3162			0.65	0.22	0.65	0.17
3217			-0.08	-0.07	-0.08	-0.08
3231			-1.17	0.15	-1.17	0.16
3242			1.22	-1.04	1.22	-1.04
3261			2.61	0.19	2.61	0.18
3324			-0.44	0.21	-0.44	0.21

#### D. Vibrational Frequencies

In Table VI, we list the vibrational frequencies computed with Hartree-Fock (HF) and the density functional theory (DFT) with the B3LYP functional and the corresponding vibrational mode assignments. The vibrational modes obtained at the HF level generally have the same assignments as those computed with DFT/B3LYP, except for modes 10–11 and 20–22. The HF frequencies

were re-ordered to align with the DFT/B3LYP assignments.

TABLE VI. Experimental and computed vibrational frequencies ( $\text{cm}^{-1}$ ) and assignments.

Mode	Exp.	HF	DFT/B3LYP	Mode Assignment (asterisk indicates the chiral center)
1	200	227	210	CH <sub>3</sub> torsion
2	360	397	372	C-C*-CH <sub>3</sub> bend + O-C*-CH <sub>3</sub> bend
3	419	442	413	O-C*-CH <sub>3</sub> bend + C-C*-CH <sub>3</sub> bend
4	742	851	771	C*-O str + C-O str + C*-CH <sub>3</sub> str
5	824	940	843	C*-O str + C*-CH <sub>2</sub> str
6	892	986	908	CH <sub>2</sub> twist
7	946	1070	972	C-O str + C*-CH <sub>3</sub> str + CH <sub>3</sub> rock
8	1020	1139	1044	CH <sub>3</sub> rock + CH <sub>2</sub> twist + C*-H bend
9	1101	1238	1133	CH <sub>2</sub> rock + CH <sub>3</sub> rock
10	1135	1296	1156	CH <sub>2</sub> wagging
11	1140	1267	1168	CH <sub>2</sub> twisting + C*-CH <sub>3</sub> str
12	1164	1310	1191	C*-H bend
13	1262	1407	1294	C*-H bend + C*-CH <sub>2</sub> str
14	1365	1526	1411	C*-H bend + CH <sub>3</sub> wagging
15	1403	1574	1439	CH <sub>2</sub> sym bend + C*-CH <sub>3</sub> str
16	1450	1600	1485	CH <sub>3</sub> asym bend
17	1460	1614	1498	CH <sub>3</sub> asym bend
18	1498	1672	1533	CH <sub>2</sub> sym bend
19		3162	3028	CH <sub>3</sub> sym str
20		3242	3082	CH <sub>2</sub> sym str
21		3217	3086	C*-H str + CH <sub>3</sub> asym str
22		3231	3088	CH <sub>3</sub> asym str
23		3261	3110	C*-H str
24		3324	3166	CH <sub>2</sub> asym str

## ACKNOWLEDGMENTS

This work was supported by the U.S. Department of Energy, Office of Science, Office of Basic Energy Sciences, under Award No. DE-SC0025393. The authors thank Nadine Bradbury, Titouan Duston, Linqing Peng, and Xuecheng Tao for useful discussion.

## REFERENCES

- <sup>1</sup>B. List, R. A. Lerner, and C. F. Barbas, “Proline-catalyzed direct asymmetric aldol reactions,” *Journal of the American Chemical Society* **122**, 2395–2396 (2000).
- <sup>2</sup>A. B. Northrup and D. W. MacMillan, “The first direct and enantioselective cross-aldol reaction of aldehydes,” *Journal of the American Chemical Society* **124**, 6798–6799 (2002).
- <sup>3</sup>C. Bolm and J. A. Gladysz, “Introduction: Enantioselective Catalysis,” *Chemical Reviews* **103**, 2761–2762 (2003).
- <sup>4</sup>G. Long, R. Sabatini, M. I. Saidaminov, G. Lakhwani, A. Rasmita, X. Liu, E. H. Sargent, and W. Gao, “Chiral-perovskite optoelectronics,” *Nature Reviews Materials* **5**, 423–439 (2020).
- <sup>5</sup>J. Crassous, M. J. Fuchter, D. E. Freedman, N. A. Kotov, J. Moon, M. C. Beard, and S. Feldmann, “Materials for chiral light control,” *Nature Reviews. Materials* **8**, 365–371 (2023).
- <sup>6</sup>J. Liu, H. Zhou, W. Yang, and K. Ariga, “Soft Nanoarchitectonics for Enantioselective Biosensing,” *Accounts of Chemical Research* **53**, 644–653 (2020).
- <sup>7</sup>L. A. Warning, A. R. Miandashti, L. A. McCarthy, Q. Zhang, C. F. Landes, and S. Link, “Nanophotonic Approaches for Chirality Sensing,” *ACS Nano* **15**, 15538–15566 (2021).
- <sup>8</sup>R. Naaman and D. H. Waldeck, “Chiral-Induced Spin Selectivity Effect,” *The Journal of Physical Chemistry Letters* **3**, 2178–2187 (2012).
- <sup>9</sup>B. P. Bloom, Z. Chen, H. Lu, and D. H. Waldeck, “A chemical perspective on the chiral induced spin selectivity effect,” *National Science Review* **11**, nwae212 (2024).
- <sup>10</sup>R. Naaman and D. H. Waldeck, “Spintronics and Chirality: Spin Selectivity in Electron Transport Through Chiral Molecules,” *Annual Review of Physical Chemistry* **66**, 263–281 (2015).
- <sup>11</sup>R. Naaman, Y. Paltiel, and D. H. Waldeck, “Chiral Induced Spin Selectivity Gives a New Twist on Spin-Control in Chemistry,” *Accounts of Chemical Research* **53**, 2659–2667 (2020).
- <sup>12</sup>Y. Sang, F. Tassinari, K. Santra, W. Zhang, C. Fontanesi, B. P. Bloom, D. H. Waldeck, J. Fransson, and R. Naaman, “Chirality enhances oxygen reduction,” *Proceedings of the National*

- Academy of Sciences **119**, e2202650119 (2022).
- <sup>13</sup>S. F. Ozturk and D. D. Sasselov, “On the origins of life’s homochirality: Inducing enantiomeric excess with spin-polarized electrons,” *Proceedings of the National Academy of Sciences* **119**, e2204765119 (2022).
- <sup>14</sup>S. F. Ozturk, D. K. Bhowmick, Y. Kapon, Y. Sang, A. Kumar, Y. Paltiel, R. Naaman, and D. D. Sasselov, “Chirality-induced avalanche magnetization of magnetite by an RNA precursor,” *Nature Communications* **14**, 6351 (2023).
- <sup>15</sup>L. D. Barron, “From Cosmic Chirality to Protein Structure: Lord Kelvin’s Legacy,” *Chirality* **24**, 879–893 (2012).
- <sup>16</sup>S. Nie and S. R. Emory, “Probing Single Molecules and Single Nanoparticles by Surface-Enhanced Raman Scattering,” *Science* **275**, 1102–1106 (1997).
- <sup>17</sup>K. Kneipp, Y. Wang, H. Kneipp, L. T. Perelman, I. Itzkan, R. R. Dasari, and M. S. Feld, “Single Molecule Detection Using Surface-Enhanced Raman Scattering (SERS),” *Physical Review Letters* **78**, 1667–1670 (1997).
- <sup>18</sup>S. Abdali and E. William Blanch, “Surface enhanced Raman optical activity ( SEROA ),” *Chemical Society Reviews* **37**, 980–992 (2008).
- <sup>19</sup>L. Barron, , and A. Buckingham, “Rayleigh and Raman scattering from optically active molecules,” *Molecular Physics* **20**, 1111–1119 (1971).
- <sup>20</sup>L. D. Barron, M. P. Bogaard, and A. D. Buckingham, “Raman scattering of circularly polarized light by optically active molecules,” *Journal of the American Chemical Society* **95**, 603–605 (1973).
- <sup>21</sup>W. Hug, S. Kint, G. F. Bailey, and J. R. Scherer, “Raman circular intensity differential spectroscopy. Spectra of (-)-.alpha.-pinene and (+)-.alpha.-phenylethylamine,” *Journal of the American Chemical Society* **97**, 5589–5590 (1975).
- <sup>22</sup>L. A. Nafie, “Adiabatic molecular properties beyond the born–oppenheimer approximation. complete adiabatic wave functions and vibrationally induced electronic current density,” *The Journal of Chemical Physics* **79**, 4950–4957 (1983).
- <sup>23</sup>L. A. Nafie, “INFRARED AND RAMAN VIBRATIONAL OPTICAL ACTIVITY: Theoretical and Experimental Aspects,” *Annual Review of Physical Chemistry* **48**, 357–386 (1997).
- <sup>24</sup>P. J. Stephens, “Theory of vibrational circular dichroism,” *The Journal of Physical Chemistry* **89**, 748–752 (1985).

- <sup>25</sup>P. J. Stephens, “Gauge dependence of vibrational magnetic dipole transition moments and rotational strengths,” *The Journal of Physical Chemistry* **91**, 1712–1715 (1987).
- <sup>26</sup>P. Stephens and F. Devlin, “Determination of the structure of chiral molecules using ab initio vibrational circular dichroism spectroscopy,” *Chirality* **12**, 172–179 (2000).
- <sup>27</sup>C. A. Mead and D. G. Truhlar, “On the determination of born–oppenheimer nuclear motion wave functions including complications due to conical intersections and identical nuclei,” *The Journal of Chemical Physics* **70**, 2284–2296 (1979).
- <sup>28</sup>M. V. Berry, “Quantal phase factors accompanying adiabatic changes,” *Proceedings of the Royal Society of London. A. Mathematical and Physical Sciences* **392**, 45–57 (1984).
- <sup>29</sup>R. Resta, “Molecular Berry curvatures and the adiabatic response tensors,” *The Journal of Chemical Physics* **158**, 024105 (2023).
- <sup>30</sup>T. Duston, Z. Tao, X. Bian, M. Bhati, J. Rawlinson, R. G. Littlejohn, Z. Pei, Y. Shao, and J. E. Subotnik, “A Phase-Space Electronic Hamiltonian For Vibrational Circular Dichroism,” *Journal of Chemical Theory and Computation* **20**, 7904–7921 (2024).
- <sup>31</sup>Z. Tao, T. Qiu, X. Bian, T. Duston, N. Bradbury, and J. E. Subotnik, “A basis-free phase space electronic Hamiltonian that recovers beyond Born–Oppenheimer electronic momentum and current density,” *The Journal of Chemical Physics* **162**, 144111 (2025).
- <sup>32</sup>Y. Wu, X. Bian, J. I. Rawlinson, R. G. Littlejohn, and J. E. Subotnik, “A phase-space semiclassical approach for modeling nonadiabatic nuclear dynamics with electronic spin,” *The Journal of Chemical Physics* **157**, 011101 (2022).
- <sup>33</sup>Z. Tao, T. Duston, Z. Pei, Y. Shao, J. Rawlinson, R. Littlejohn, and J. E. Subotnik, “An electronic phase-space Hamiltonian approach for electronic current density and vibrational circular dichroism,” *The Journal of Chemical Physics* **161**, 204107 (2024).
- <sup>34</sup>M. Bhati, Z. Tao, X. Bian, J. Rawlinson, R. Littlejohn, and J. E. Subotnik, “A Phase-Space Electronic Hamiltonian for Molecules in a Static Magnetic Field. I: Conservation of Total Pseudomomentum and Angular Momentum,” *The Journal of Physical Chemistry A* **129**, 4555–4572 (2025).
- <sup>35</sup>M. Bhati, Z. Tao, X. Bian, J. Rawlinson, R. Littlejohn, and J. E. Subotnik, “A Phase-Space Electronic Hamiltonian for Molecules in a Static Magnetic Field II: Quantum Chemistry Calculations with Gauge Invariant Atomic Orbitals,” *The Journal of Physical Chemistry A* **129**, 4573–4590 (2025).

- <sup>36</sup>R. D. Amos, “Electric and magnetic properties of CO, HF, HCl, and CH<sub>3</sub>F,” *Chemical Physics Letters* **87**, 23–26 (1982).
- <sup>37</sup>G. Placzek, *The Rayleigh and Raman scattering*, UCRL-526(L (University of California, Radiation Laboratory, Berkeley, Calif., 1959).
- <sup>38</sup>Y. Cornaton, M. Ringholm, O. Louant, and K. Ruud, “Analytic calculations of anharmonic infrared and Raman vibrational spectra,” *Physical Chemistry Chemical Physics* **18**, 4201–4215 (2016).
- <sup>39</sup>S. Lubber, “Raman Optical Activity Spectra from Density Functional Perturbation Theory and Density-Functional-Theory-Based Molecular Dynamics,” *Journal of Chemical Theory and Computation* **13**, 1254–1262 (2017).
- <sup>40</sup>Q. Yang, J. Kapitán, P. Bouř, and J. Bloino, “Anharmonic Vibrational Raman Optical Activity of Methyloxirane: Theory and Experiment Pushed to the Limits,” *The Journal of Physical Chemistry Letters* (2022), 10.1021/acs.jpcclett.2c02320.
- <sup>41</sup>D. Rappoport and F. Furche, “Lagrangian approach to molecular vibrational Raman intensities using time-dependent hybrid density functional theory,” *The Journal of Chemical Physics* **126**, 201104 (2007).
- <sup>42</sup>T. D. Crawford and K. Ruud, “Coupled-Cluster Calculations of Vibrational Raman Optical Activity Spectra,” *ChemPhysChem* **12**, 3442–3448 (2011).
- <sup>43</sup>K. H. Hopmann, K. Ruud, M. Pecul, A. Kudelski, M. Dračinský, and P. Bouř, “Explicit versus Implicit Solvent Modeling of Raman Optical Activity Spectra,” *The Journal of Physical Chemistry B* **115**, 4128–4137 (2011).
- <sup>44</sup>S. T. Mutter, F. Zielinski, P. L. A. Popelier, and E. W. Blanch, “Calculation of Raman optical activity spectra for vibrational analysis,” (2015), 10.1039/C4AN02357A.
- <sup>45</sup>K. Ruud and A. J. Thorvaldsen, “Theoretical approaches to the calculation of Raman optical activity spectra,” *Chirality* **21**, E54–E67 (2009).
- <sup>46</sup>J. R. Cheeseman and M. J. Frisch, “Basis Set Dependence of Vibrational Raman and Raman Optical Activity Intensities,” *Journal of Chemical Theory and Computation* **7**, 3323–3334 (2011).
- <sup>47</sup>J. R. Escribano, T. B. Freedman, and L. A. Nafie, “Bond polarizability and vibronic coupling theories of Raman optical activity: The electric-dipole magnetic-dipole optical activity tensor,” *The Journal of Chemical Physics* **87**, 3366–3374 (1987).
- <sup>48</sup>L. D. Barron, A. R. Gargaro, L. Hecht, and P. L. Polavarapu, “Experimental and *ab initio* theoretical vibrational Raman optical activity of alanine,” *Spectrochimica Acta Part A: Molecular*

- Spectroscopy **47**, 1001–1016 (1991).
- <sup>49</sup>P. L. Polavarapu, “Ab initio vibrational Raman and Raman optical activity spectra,” *The Journal of Physical Chemistry* **94**, 8106–8112 (1990).
- <sup>50</sup>L. A. Nafie, “Adiabatic molecular properties beyond the Born–Oppenheimer approximation. Complete adiabatic wave functions and vibrationally induced electronic current density,” *The Journal of Chemical Physics* **79**, 4950–4957 (1983).
- <sup>51</sup>S. Patchkovskii, “Electronic currents and born-oppenheimer molecular dynamics,” *The Journal of Chemical Physics* **137** (2012), 10.1063/1.4747540.
- <sup>52</sup>M. Okuyama and K. Takatsuka, “Electron flux in molecules induced by nuclear motion,” *Chemical Physics Letters* **476**, 109–115 (2009).
- <sup>53</sup>X. Bian, Z. Tao, Y. Wu, J. Rawlinson, and J. E. S. Robert G Littlejohn, “Total angular momentum conservation in ab initio born-oppenheimer molecular dynamics,” *Phys. Rev. B* **108**, L220304 (2023).
- <sup>54</sup>B. Barrera, D. P. Arovas, A. Chandran, and A. Polkovnikov, “The moving born-oppenheimer approximation,” arXiv preprint arXiv:2502.17557 (2025).
- <sup>55</sup>Z. Tao, T. Qiu, M. Bhati, X. Bian, T. Duston, J. Rawlinson, R. G. Littlejohn, and J. E. Subotnik, “Practical phase-space electronic Hamiltonians for ab initio dynamics,” *The Journal of Chemical Physics* **160**, 124101 (2024).
- <sup>56</sup>N. Shenvi, “Phase-space surface hopping: Nonadiabatic dynamics in a superadiabatic basis,” *The Journal of Chemical Physics* **130**, 124117 (2009).
- <sup>57</sup>X. Wu, X. Bian, J. Rawlinson, R. G. Littlejohn, and J. E. Subotnik, “Recovering Exact Vibrational Energies within a Phase Space Electronic Structure Framework,” *Journal of Chemical Theory and Computation* **21**, 9470–9482 (2025).
- <sup>58</sup>R. Littlejohn, J. Rawlinson, and J. Subotnik, “Representation and conservation of angular momentum in the born–oppenheimer theory of polyatomic molecules,” *The Journal of Chemical Physics* **158**, 104302 (2023).
- <sup>59</sup>S. B. Schneiderman and A. Russek, “Velocity-dependent orbitals in proton-on-hydrogen-atom collisions,” *Physical Review* **181**, 311–321 (1969).
- <sup>60</sup>S. Fatehi, E. Alguire, Y. Shao, and J. E. Subotnik, “Analytic derivative couplings between configuration-interaction-singles states with built-in electron-translation factors for translational invariance,” *The Journal of Chemical Physics* **135**, 234105 (2011).

- <sup>61</sup>V. Athavale, X. Bian, Z. Tao, Y. Wu, T. Qiu, J. Rawlinson, R. G. Littlejohn, and J. E. Subotnik, “Surface hopping, electron translation factors, electron rotation factors, momentum conservation, and size consistency,” *The Journal of Chemical Physics* **159** (2023), 10.1063/5.0160965.
- <sup>62</sup>T. Qiu, M. Bhati, Z. Tao, X. Bian, J. Rawlinson, R. G. Littlejohn, and J. E. Subotnik, “A simple one-electron expression for electron rotational factors,” *The Journal of Chemical Physics* **160**, 124102 (2024).
- <sup>63</sup>P. Schmelcher, L. S. Cederbaum, and H.-D. Meyer, “Electronic and nuclear motion and their couplings in the presence of a magnetic field,” *Phys. Rev. A* **38**, 6066–6079 (1988).
- <sup>64</sup>P. Schmelcher, L. S. Cederbaum, and H.-D. Meyer, “On the validity of the Born-Oppenheimer approximation in magnetic fields,” *Journal of Physics B: Atomic, Molecular and Optical Physics* **21**, L445 (1988).
- <sup>65</sup>L. Yin and C. Alden Mead, “Magnetic screening of nuclei by electrons as an effect of geometric vector potential,” *The Journal of chemical physics* **100**, 8125–8131 (1994).
- <sup>66</sup>R. Resta, “Manifestations of Berry’s phase in molecules and condensed matter,” *Journal of Physics: Condensed Matter* **12**, R107 (2000).
- <sup>67</sup>D. Ceresoli, “Electron-corrected Lorentz forces in solids and molecules in a magnetic field,” *Physical Review B* **75** (2007), 10.1103/PhysRevB.75.161101.
- <sup>68</sup>T. Culpitt, L. D. M. Peters, E. I. Tellgren, and T. Helgaker, “Ab initio molecular dynamics with screened Lorentz forces. I. Calculation and atomic charge interpretation of Berry curvature,” *The Journal of Chemical Physics* **155**, 024104 (2021).
- <sup>69</sup>K. L. Bak, S. P. A. Sauer, J. Oddershede, and J. F. Ogilvie, “The vibrational g-factor of dihydrogen from theoretical calculation and analysis of vibration-rotational spectra,” *Physical Chemistry Chemical Physics* **7**, 1747–1758 (2005).
- <sup>70</sup>A. T. Ekstrøm and S. P. A. Sauer, “A Computational Study of the Vibrational and Rotational g-Factors of the Diatomic Molecules LiH, LiF, CO, CS, SiO, and SiS,” *Journal of Chemical Theory and Computation* **21**, 8876–8888 (2025).
- <sup>71</sup>P. K. Bose, P. L. Polavarapu, L. D. Barron, and L. Hecht, “Ab initio and experimental Raman optical activity in (+)-(R)-methyloxirane,” *The Journal of Physical Chemistry* **94**, 1734–1740 (1990).
- <sup>72</sup>P. L. Polavarapu, L. Hecht, and L. D. Barron, “Vibrational Raman optical activity in substituted oxiranes,” *The Journal of Physical Chemistry* **97**, 1793–1799 (1993).
- <sup>73</sup>P. Pulay and J. F. Hinton, “Shielding theory: Giau method,” *eMagRes* (2007).

- <sup>74</sup>T. Helgaker and P. Jorgensen, “An electronic hamiltonian for origin independent calculations of magnetic properties,” *The Journal of chemical physics* **95**, 2595–2601 (1991).
- <sup>75</sup>N. Nagaosa, “Anomalous Hall effect,” *Reviews of Modern Physics* **82**, 1539–1592 (2010).
- <sup>76</sup>Y. Ando, “Topological Insulator Materials,” *Journal of the Physical Society of Japan* **82**, 102001 (2013).
- <sup>77</sup>H. N. S. Krishnamoorthy, A. M. Dubrovkin, G. Adamo, and C. Soci, “Topological Insulator Metamaterials,” *Chemical Reviews* **123**, 4416–4442 (2023).
- <sup>78</sup>L. Zhang and Q. Niu, “Angular Momentum of Phonons and the Einstein–de Haas Effect,” *Physical Review Letters* **112**, 085503 (2014).
- <sup>79</sup>S. Ren, J. Bonini, M. Stengel, C. E. Dreyer, and D. Vanderbilt, “Adiabatic Dynamics of Coupled Spins and Phonons in Magnetic Insulators,” *Physical Review X* **14**, 011041 (2024).
- <sup>80</sup>F. G. Hernandez, A. Baydin, S. Chaudhary, F. Tay, I. Katayama, J. Takeda, H. Nojiri, A. K. Okazaki, P. H. Rappl, E. Abramof, M. Rodriguez-Vega, G. A. Fiete, and J. Kono, “Observation of interplay between phonon chirality and electronic band topology,” *Science Advances* **9**, eadj4074 (2023).
- <sup>81</sup>J. Fransson, “Chiral phonon induced spin polarization,” *Physical Review Research* **5**, L022039 (2023).
- <sup>82</sup>X. Li, J. Zhong, J. Cheng, H. Chen, H. Wang, J. Liu, D. Sun, L. Zhang, and J. Zhou, “Chiral phonon activated spin Seebeck effect in chiral materials,” *Science China Physics, Mechanics & Astronomy* **67**, 237511 (2024).